

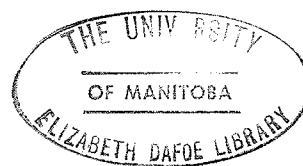
CRYSTAL STRUCTURE ANALYSIS OF
WODGINITE FROM BERNIC LAKE
MANITOBA

A Thesis
Submitted to
The Faculty of Graduate Studies
University of Manitoba

In Partial Fulfillment
of the Requirements for the
Degree, Master of Science

by
Margaret Elphick

1972



ABSTRACT

A crystal structure analysis using densitometer-measured intensities for 190 reflections recorded on an integrated precession instrument, has been carried out for a wodginite from Bernic Lake, Manitoba. The mineral is monoclinic, and the specimen analysed has true cell dimensions $a=9.516 \text{ \AA}$, $b=11.452 \text{ \AA}$ and $c=5.112 \text{ \AA}$, $\beta=91^\circ 08'$ and space group $C2/c$, but it has a strong sub-cell with $a'=4.758 \text{ \AA}$, $b'=5.726 \text{ \AA}$, $c'=5.112 \text{ \AA}$, $\beta=91^\circ 08'$ and space group $P2/c$, with cell content

$Z = 1 \times [(\text{Mn}_{0.77}^{+2} \text{Fe}_{0.25}^{+3} \text{Sn}_{0.61}^{+4} \text{Ti}_{0.35}^{+4} \text{Nb}_{0.04}^{+5} \text{Ta}_{1.98}^{+5})\text{O}_8^{-2}]$. The structure analysis described here is based on the small sub-cell.

The starting structure was based on one third of the unit cell of the columbite-tantalite structure (Sturdivant, 1930). The structure was analysed by least squares and Fourier analyses. A final structure, which was similar to that of tantalite apart from some variation in the oxygen positions, was obtained which gave an R factor of 10.5%.

In the sub-cell used for the structure analysis all the Ta atoms are ordered into one 2-fold metal site, M_1 , and the other metal atoms are in the other 2-fold metal site, M_2 . The eight oxygen atoms are in two 4-fold general positions. Both metal sites are pseudo-octahedrally coordinated by oxygens with $M_1(\text{Ta})\text{-O}$ distances from 1.908 to 2.129 \AA , and $M_2\text{-O}$ from 1.948 to 2.203 \AA , O-O distances around $M_1(\text{Ta})$ vary from 2.532 to 2.924 \AA , and around M_2 from 2.792 to 2.966 \AA .

TABLE OF CONTENTS

<u>Chapter</u>	<u>Page</u>
ABSTRACT	ii
ACKNOWLEDGEMENTS	viii
CHAPTER I - INTRODUCTION	1
1) Historical Data and Localities.	1
2a) Objectives of the Present Study.	1
2b) Relationship of Wodginite to Tantalite and Pseudo-ixiolite.	1
3) Sub-cell Content of Wodginite.	3
4) The Starting Structure for Wodginite the Structure of Columbite.	5
CHAPTER II - COLLECTION OF INTENSITY DATA	8
1) Selection of Crystal.	8
2) Determination of Cell Dimensions.	8
3) Collection of Photographic Intensity Data.	9
4) Density Measurement.	16
CHAPTER III - PROCESSING OF DATA	20
1) 'Predproc' - (Precession Processing). Processing of Intensities from Precession Photographs to Give a set of Relative Intensities.	20
2) 'Dataps' - (Data Processing). Data Reduction of the Relative Intensities to Give a Set of Relative $ F_{obs} $ Values.	22
3) 'Genles' - (General Least Squares). Structure	

<u>Chapter</u>	<u>Page</u>
Factor Calculations and Refinement of Parameters by Least Squares.	26
4) 'Fourier'- Calculation of F_0 and ΔF Fourier Syntheses.	29
CHAPTER IV - THE STRUCTURE ANALYSIS	36
1) The Starting Structure from that of Columbite-tantalite.	36
2) Solution of the Structure.	39
CHAPTER V - SUMMARY AND CONCLUSIONS	58
1) Summary.	58
2) Conclusions.	59
3) Recommendations.	59
APPENDIX I - DERIVATION OF ABSORPTION CORRECTIONS	60
APPENDIX II - DETERMINATION OF ACCURATE CELL DIMENSIONS BY THE PRECESSION METHOD	63
APPENDIX III - INPUT FORMAT FOR COMPUTER DATA	65
1) 'Precproc'.	65
2) 'Dataps'.	67
3) 'Genles'.	70
4) 'Fourier'.	74
REFERENCES	76

LIST OF TABLES

<u>Table</u>	<u>Page</u>
TABLE I - MICROPROBE ANALYSES AND NUMBERS OF CATIONS FOR WODGINITE, TANTALITE AND PSEUDO-IXIOLITE	2
TABLE II - COMPARABLE UNIT CELL DATA FOR WODGINITE, TANTALITE AND PSEUDO-IXIOLITE	4
TABLE III - CELL DIMENSIONS OF WODGINITE DERIVED BY X-RAY POWDER DIFFRACTION AND PRECESSION METHODS	10
TABLE IV - EXAMPLE OF OUTPUT DATA FROM PROGRAM 'PRECPROC'	23
TABLE V - EXAMPLE OF OUTPUT DATA FROM PROGRAM 'DATAPS'	27
TABLE VI- FINAL F_o 'S AND F_c 'S FOR ALL REFLECTIONS	30
TABLE VII - FINAL ATOMIC PARAMETERS	48
TABLE VIII - BOND LENGTHS	56
TABLE IX - INTERBOND LENGTHS	57
TABLE AI.1 - CALCULATION OF LINEAR-ABSORPTION COEFFICIENT FOR WODGINITE	62

LIST OF FIGURES

<u>Figure</u>	<u>Page</u>
Figure 1a. Crystal Structure of Tantalite as Determined by Sturdivant, 1930.	6
Figure 1b. Structure Model I for Wodginite.	7
Figure 2. Apparatus used for Simultaneously Developing Four or Five Precession Photographs.	17
Figure 4. Electron Density Maps (F_o Syntheses) from Model I.	
a) x y section at $z = 0.25$.	41
b) x y section at $z = 0.45$	42
Figure 5. Difference Maps (ΔF Syntheses) from Model I.	
a) x y section at $z = 0.10$.	43
b) x y section at $z = 0.05$.	44
Figure 6. Final Electron Density Maps (F_o Syntheses)	
a) x y section at $z = 0.25$.	50
b) x y section at $z = 0.10$.	51
c) x y section at $z = 0.05$.	52
Figure 7. Final Difference Maps (ΔF Syntheses)	
a) x y section at $z = 0.25$.	53
b) x y section at $z = 0.10$.	54
Figure 8. Projection Along y of the Final Structure of Wodginite	55

LIST OF PLATES

<u>Plate</u>	<u>Page</u>
PLATE Ia - 0-LEVEL PRECESSION PHOTOGRAPH ABOUT \underline{y} [010]	12
PLATE Ib - 1ST-LEVEL PRECESSION PHOTOGRAPH ABOUT \underline{y} [010]	13
PLATE II - 0-LEVEL INTEGRATED PRECESSION PHOTOGRAPH ABOUT \underline{x} [100]	14

ACKNOWLEDGEMENTS

The author would like to acknowledge the following people for their help, either directly or indirectly, in this study: at the University of Manitoba, Dr. R.B. Ferguson, Professor of Mineralogy in the Department of Earth Sciences under whose supervision this study was carried out and whose help was most valuable; Mr. Joel Grice, graduate student in the same Department, for making wadginite specimens of his from a former study available and for calculating bond lengths and bond angles for this structure after the author had left the laboratory; Dr. W. Kaufman of the Department of Oral Biology, Faculty of Dentistry, for the loan of an integrating precession camera and for advice in its use, also for making available the two computer programs 'Precproc' and 'Dataps'. The author would also like to thank from outside the University of Manitoba Dr. Anne Kerr, of the Department of Chemistry, University of Calgary, for adaptations of A.C. Larson's programs 'Genles' and 'Fourier' for use with an I.B.M. 360/65 computer and for making them available to the author's laboratory. Thanks are also due to Dr. Larson of the United States Atomic Energy Commission, Los Alamos, New Mexico, for indirectly providing these programs. Finally she wants to acknowledge financial support in the form of research grants to Dr. Ferguson from the National Research Council of Canada, and the Geological Survey of Canada.

CHAPTER I
INTRODUCTION

1) Historical Data and Localities.

Wodginite is named after the town of Wodgina in Australia, the locality where it was first discovered. It was originally thought to be a tin-manganese tantalite, called pseudo-ixiolite, but was recognised as a new mineral by Nickel, Rowland and McAdam in 1963. They also described it from the Chemalloy (Tanco) pegmatite at Bernic Lake, Manitoba, and it is the wodginite from this area that is the subject of the crystal structure analysis described here.

In addition to the two original occurrences of wodginite described by Nickel et al (1963), several others have been discovered since: Rwanda, Belgium Congo (Bourguignon and Melon, 1965); Krasonice, Moravia (Luna, 1965); Kablin Range, U.S.S.R. (Khvostova et al, 1965); Sukula, Tammela, S.W. Finland (Vorma and Siivola, 1967); Karibib, Southwest Africa, (von Knorring, 1968); and Ankole, S.W. Uganda (von Knorring, Sahama and Lehtinen, 1969).

2a) Objectives of the Present Study.

(a) To analyse the structure so that it is known for its own sake and thus to show whether it is essentially isostructural with tantalite as the crystallographic evidence suggests, and (b) to see if there is any evidence of ordering of the metal atoms.

2b) Relationship of Wodginite to Tantalite and Pseudo-ixiolite.

As Grice (1970) and Grice, Cerny and Ferguson (1972) have shown in a detailed study of wodginite and related minerals from the Tanco pegmatite, Bernic Lake, Manitoba, the wodginite there is closely related chemically to the associated tantalite (see Table I). It may be seen that wodginite is mainly richer in SnO_2 , Ta_2O_5 and FeO and poorer

TABLE I
MICROPROBE ANALYSES AND NUMBERS OF CATIONS
FOR WODGINITE, TANTALITE AND PSEUDO-IXIOLITE

	<u>Analyses in Weight Percent</u>		
	<u>Wodginite</u> ¹	<u>Tantalite</u> ²	<u>Pseudo-ixiolite</u> ³
MnO	9.2	14.1	14.7
FeO	3.0	0.4	0.2
SnO ₂	15.5	0.4	0.8
TiO ₂	1.3	0.8	1.0
Ta ₂ O ₅	73.3	67.6	64.2
Nb ₂ O ₅	<u>1.0</u>	<u>17.6</u>	<u>20.1</u>
	103.3	100.9	101.0

	<u>Numbers of Cations on the Basis of 32 Oxygens</u>		
Mn ⁺²	3.09	3.59	3.68
Fe ⁺²	0.99	0.09	0.06
Sn ⁺⁴	2.45	0.04	0.16
Ti ⁺⁴	1.40	0.14	0.23
Ta ⁺⁵	7.91	5.59	5.14
Nb ⁺⁵	<u>0.18</u>	<u>2.43</u>	<u>2.69</u>
	16.02	11.85	11.96

These analyses are taken from Grice (1970) and from Grice et al (1972), the analyst was Mr. S. Jones, Nuclear Research Establishment, Pinawa, Manitoba. 1 - sample number G - 69 - 17 in Grice (1970); 2 - mean of four analyses (Table 3, Grice et al, 1972); 3 - mean of 5 analyses (Table 4, Grice et al, 1972).

in MnO and Nb₂O₅ than is tantalite-pseudo-ixiolite.

Nickel et al (1963) and Grice (1970) and Grice et al (1972) have shown that wodginite, tantalite and pseudo-ixiolite are closely related to each other not only chemically but also crystallographically. These relationships are discussed by the above authors, and are summarised in Table II (taken from Grice et al, 1972, Table 5). The facts relevant to the present structure are that, whereas tantalite and pseudo-ixiolite are both orthorhombic with space group Pbcn, wodginite is monoclinic C2/c or Cc and with $\beta \sim 91^\circ$. Also, and of importance, tantalite has true cell dimensions of approximately $a = 3 \times 4.80 \text{ \AA}$, $b = 5.76 \text{ \AA}$, $c = 5.11 \text{ \AA}$, whereas wodginite has (true) values of $a = 9.50 \text{ \AA}$, two thirds that of tantalite, $b = 11.45 \text{ \AA}$, twice that of tantalite and $c = 5.11 \text{ \AA}$, the same as that of tantalite. The cell of wodginite is discussed further below.

The densities of both wodginite and tantalite are similar, The calculated density for a Tanco wodginite is 7.75 gm/cc. and the observed for one of the Tanco tantalites is 6.76 gm/cc. Whereas wodginite generally forms poor crystals and is dark brown to grey in colour, tantalite commonly forms good crystals which are black; however, with many specimens it is not possible to distinguish the two minerals by eye observation alone.

3) Sub-cell and Cell Content of Wodginite.

The (true) unit cell of wodginite described above has a cell content of $1 \times [(\text{Mn}_{3.09}^{+2} \text{Fe}_{0.99}^{+3} \text{Sn}_{2.45}^{+4} \text{Ti}_{1.40}^{+4} \text{Nb}_{0.18}^{+5} \text{Ta}_{7.91}^{+5})_{32}^{0-2}]$ (Table I). This content relates to the true cell for wodginite but this cell is only distinguished on X-ray diffraction photographs by very weak reflections. The photographs are dominated by a strong sub-cell with, as Table II shows, $a' = 4.75 \text{ \AA} = a/2$, $b' = 5.72 \text{ \AA} = b/2$, and $c' = 5.11 \text{ \AA} = c$, $\beta' = \beta \sim 91^\circ$, $V' = 139 \text{ \AA}^3 = V/4$, space group P2/c or Pc and $Z' = Z/4$.

Because of the difficulty, described in the next Chapter, of recording the weak reflections characteristic of wodginite's true cell, these weak reflections were ignored in the present study, and the other reflections were indexed on the sub-cell. The structure analysis of

TABLE II
COMPARABLE UNIT CELL DATA FOR WODGINITE,
TANTALITE AND PSEUDO-IXIOLITE

This table is modified after Table 5 of Grice et al (1972). The settings are those of Strunz and Tennyson (1970) adopted by Grice et al (1972).

	<u>Pseudo-ixiolite</u>	<u>Tantalite</u>		<u>Wodginite</u>	
		<u>true</u>	<u>sub</u>	<u>true</u>	<u>sub</u>
Axial	<u>a</u> 4.76	<u>a</u> 14.40	<u>a/3</u> 4.80	<u>a</u> 9.50	<u>a/2</u> 4.75
Lengths, Å	<u>b</u> 5.75	<u>b</u> 5.76	(<u>b</u>) -	<u>b</u> 11.45	<u>b/2</u> 5.72
	<u>c</u> 5.16	<u>c</u> 5.11	(<u>c</u>) -	<u>c</u> 5.11	(<u>c</u>) -
β	(90°)	(90°)	(90°)	91°	91°
$V, \text{Å}^3$	141	423	1/3 423=141	557	1/4 556=139
Space Group	<u>Pbcn</u>	<u>Pbcn</u>	<u>Pbcn</u>	<u>C2/cor Cc</u>	<u>P2/c or Pc</u>
Ideal Cell	(A,B) ₄ O ₈	A ₄ B ₈ O ₂₄	1/3[A ₄ B ₈ O ₂₄]	A ₈ B ₈ O ₃₂ *	1/4[A ₈ B ₈ O ₃₂]
Content**					

* Evidence is given in this thesis for the ordering of the Ta atoms into one site in wodginite, and so the formula is here written accordingly.

** A = Fe, Mn(+>> Sn, Ti); B = Nb, Ta, (+ Sn, Ti)

wodginite described in this thesis thus relates to the sub-cell with one quarter the volume of the true cell, and with the following approximate dimensions, symmetry and cell content (where we now use unprimed symbols to describe the cell used for the analysis):

$$\underline{a} = 4.75, \underline{b} = 5.72, \underline{c} = 5.11 \text{ \AA}, \beta \sim 91^\circ;$$

$$\underline{V} = 139 \text{ \AA}^3; \text{ space group } \underline{F2/c} \text{ or } \underline{Pc}, Z = A_2B_2O_8 = 2[ABC_4];$$

$$Z = 1 \times [(\text{Mn}^{+2}_{0.77} \text{Fe}^{+3}_{0.25} \text{Sn}^{+4}_{0.61} \text{Ti}^{+4}_{0.35} \text{Nb}^{+5}_{0.04} \text{Ta}^{+5}_{1.98})O_8^{-2}]$$

4) The Starting Structure for Wodginite: the Structure of Columbite.

Because of the close similarity of wodginite to tantalite, and hence to columbite, with respect to unit cell dimensions, chemistry and cell content (Tables I and II), and also with respect to X-ray powder diffraction patterns (Nickel et al, 1963; Grice, 1970), it is reasonable to assume that the crystal structure of wodginite is similar to that of columbite-tantalite. For this reason, the starting positions chosen for the atoms in our analysis of wodginite were those given by Sturdivant (1930) for columbite. Sturdivant's structure for columbite is shown in Fig. 1a and the corresponding starting structure for wodginite (Model I) is shown in Fig. 1b. The relationship between the cell of wodginite adopted here and that of columbite used by Sturdivant is as follows:

<u>Wodginite</u> (this study)	<u>Approximate</u> period, \AA	<u>Columbite</u> (Sturdivant, 1930)
<u>a</u>	4.7	<u>a/3</u>
<u>b</u>	5.7	<u>b</u>
<u>c</u>	5.1	<u>c</u>

Figure 1a. Crystal Structure of tantalite as determined by

Sturdivant (1930)

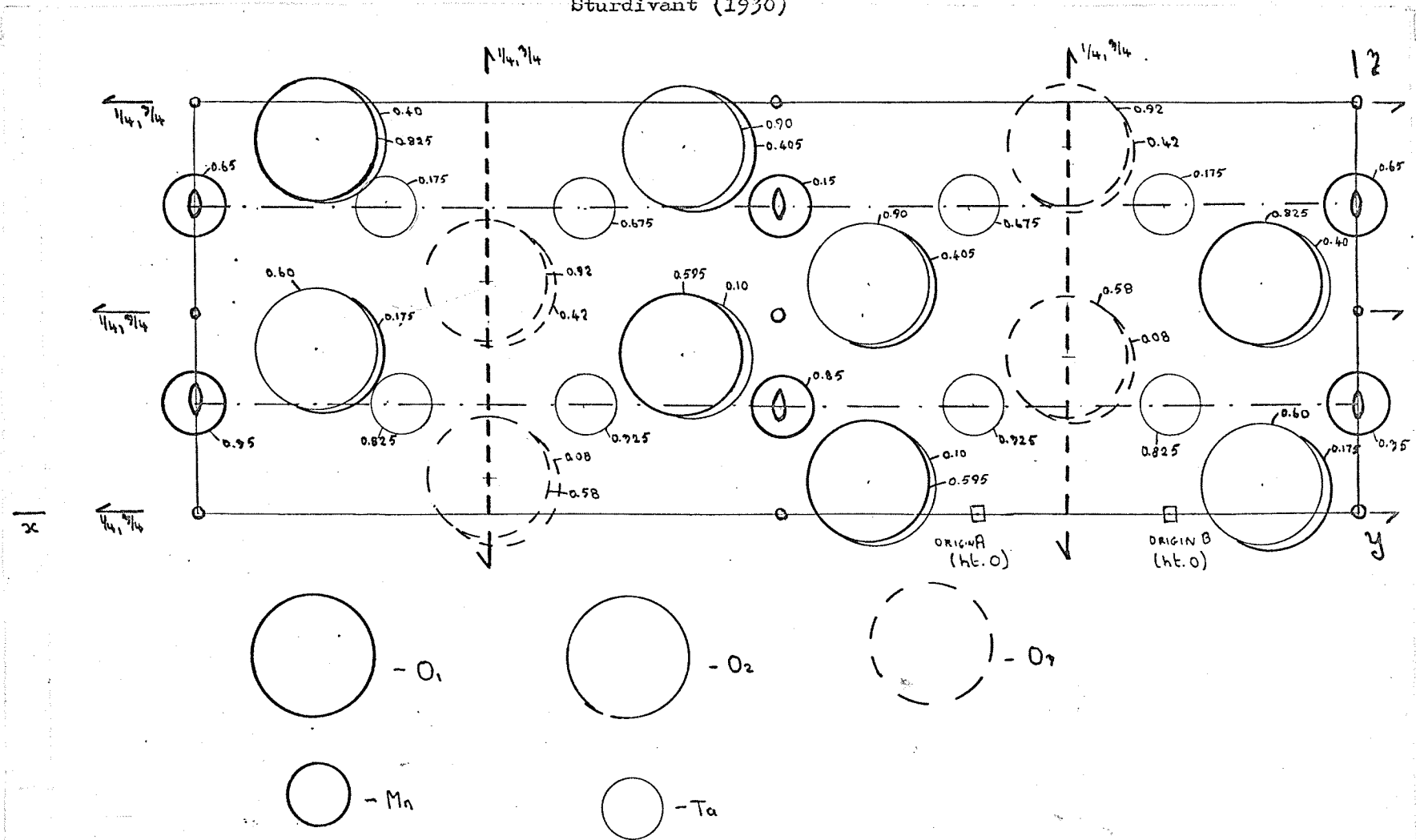
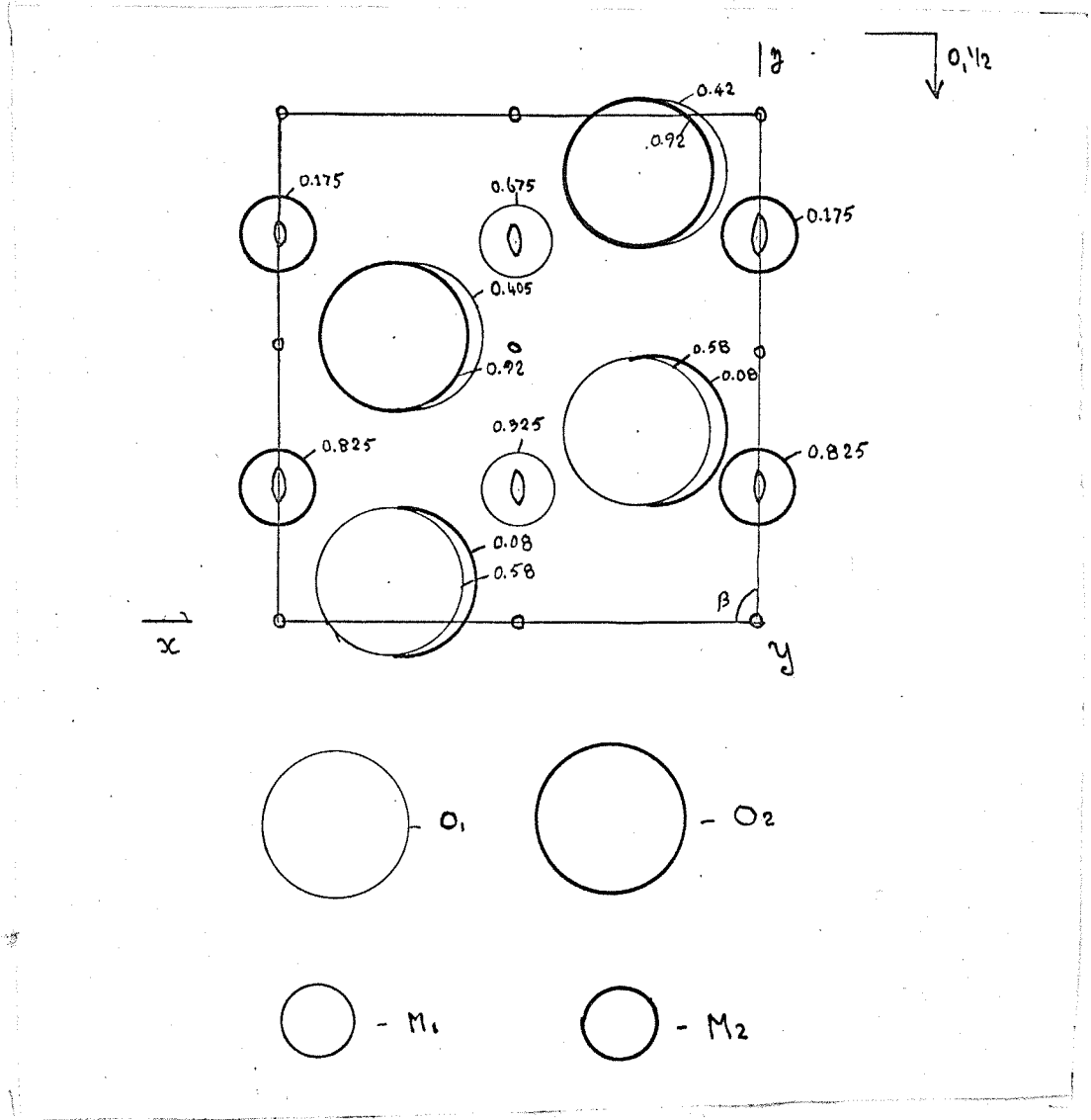


Figure 1b. Structure Model I for
wodginite



CHAPTER IICOLLECTION OF INTENSITY DATA1) Selection of Crystal.

The samples of wodginite available were those used in a mineralogical study by Grice (1970) of wodginite and related minerals from the Tantalum Mining Corporation of Canada (Tanco) mine at Bernic Lake, Manitoba. Consequently, chemical analyses and crystallographic data were already available for these particular samples.

Several crystals from different specimens of Grice's (1970) were mounted and oriented with the Buerger precession camera. Zero- and upper-level photographs were taken to investigate the suitability of the crystals for use in the structure analysis. The crystals from one specimen in particular, Grice's specimen no. G-69-17, showed less tendency than others to be multiply grown.

A single crystal from this sample was consequently ground to a sphere, remounted, and oriented with the precession camera so that it rotated about the z^* axis. The purpose in using a spherical crystal was to simplify corrections for the X-rays absorbed during the passage of the X-ray beam through the crystal. The crystal was also made as small as possible in order to minimise the absorption correction.

(For a more comprehensive explanation of absorption see Appendix I).

2) Determination of Cell Dimensions.

While it is generally thought that the precession camera is one of the least accurate instruments with which to determine cell dimensions it has been pointed out by several authors (Barnes, Przybylska and Shore, 1951; Barnes, 1949; Patterson and Love, 1960.) that providing allowance is made for film shrinkage and providing the camera is standardised with a crystal of

known and constant cell dimensions such as quartz, then the accuracy that can be obtained by this method is sufficient to enable the results to be used in a structure analysis. For a description of the procedures for deriving fairly accurate cell dimensions from precession photographs, see Appendix II.

Accordingly, the precession camera was standardised using the $(11\bar{2}1)$ reflection of quartz, and thus the accurate effective crystal- to- film distance calculated. The cell dimensions of the chosen wadginite were then calculated from zero- and first-level photographs precessing around both the x and the y axes. The results obtained were then recalculated to allow for film shrinkage in a manner described in Appendix II.

The final results are compared in Table III with the cell dimensions obtained for the same specimen (but not the same actual material) by Grice (1970) using X-ray powder diffraction data. It can be seen from Table III that the accuracy obtained by the powder diffraction method is much greater than that obtained by the precession method so that in all ensuing calculations the more accurate powder values were used.

3) Collection of Photographic Intensity Data.

In this investigation, the reflections were recorded on an integrating precession instrument, and the intensities measured using a densitometer. The instrument used to record the data was manufactured by the Charles Supper Co., and was on loan from Dr. W. Kaufman of the Department of Oral Biology, Faculty of Dentistry of the University of Manitoba. No one with first-hand experience in the use of an integrating precession camera for the structure analysis of minerals was readily available for consultation, but Dr. Kaufman (in a different laboratory from the writer, and several miles away) had used a similar

TABLE III
CELL DIMENSIONS OF WODGINITE DERIVED BY
X-RAY POWDER DIFFRACTION AND PRECESSION
CAMERA METHODS

The cell dimensions refer to the sub-cell which was used for the structure analysis.

	<u>Powder Method</u>	<u>Precession Method</u>
	<u>(Grice, 1970)</u>	<u>(this study)</u>
<u>a</u> , Å	4.758 ± 0.002	4.803 ± 0.032
<u>b</u> , Å	5.726 ± 0.002	5.719 ± 0.023
<u>c</u> , Å	5.112 ± 0.002	5.095 ± 0.018
β	91°08' ± 05'	n.d.

NOTE: The cell dimensions on the left, those determined by the powder method, were used in this structure analysis.

instrument quite successfully several times for the structure analysis of biochemicals, and he provided some help periodically.

A full description of the geometry of the precession camera and of the procedures to be followed in its use are given in books such as those by Buerger (1964) and by Nuffield (1966). Plates Ia and Ib are typical 0- and 1-level precession photographs.

A description of the integrating procedure for the precession camera is given in Buerger (1960) on page 89. Plate II shows a typical 0-level integrated precession photograph. It can be seen that each spot on this photograph is of uniform size and is of uniform intensity as compared with the irregular shape and intensity of the spots in the non-integrated photograph shown in Plate Ia.

From the descriptions of the precession method given in the references just quoted, it is clear that the larger the repeat period of the direct lattice along the precession axis, the more levels that can be recorded about this axis within the limited range of movement imposed on the film cassette by the mechanics of the camera. When the integrating mechanism of the camera is brought into play, the range of movement of the film cassette is further limited. While this has no serious effect in limiting the number of reflections that can be recorded in crystals with a large repeat period ($> \sim 14 \text{ \AA}$) such as biochemicals, etc., in wodginite with repeat periods of $\sim 5 \text{ \AA}$, it limited the number of upper levels recordable about both the x and the y axes to a maximum of only two, using integrating methods. Thus it was not possible to record with any degree of accuracy the high $\sin\theta$ reflections so essential to the sensitivity of a structure analysis.

PLATE IaC-LEVEL PRECESSION PHOTOGRAPHABOUT $y[010]$

Radiation Mo/Zn, $\bar{\mu} = 25^\circ$, $r_s = 15$ mm., $s = 32$ mm., $F = 60$ mm.,
 rotation axis $z [001]$.

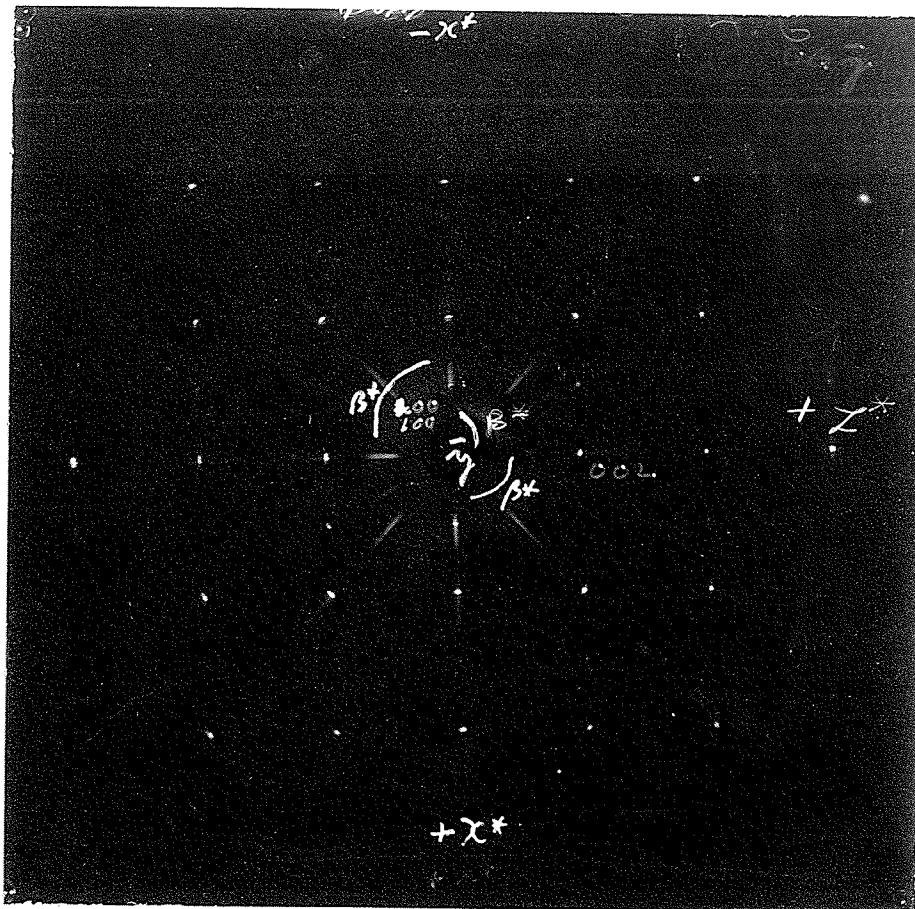


PLATE Ib1ST-LEVEL PRECESSION PHOTOGRAPHABOUT $y[010]$

Radiation Mo/Zn, $\bar{\mu} = 25^\circ$, $r_s = 25$ mm., $s = 32.5$ mm., $F.d^* = 7.5$ mm.,
rotation axis $z [001]$.

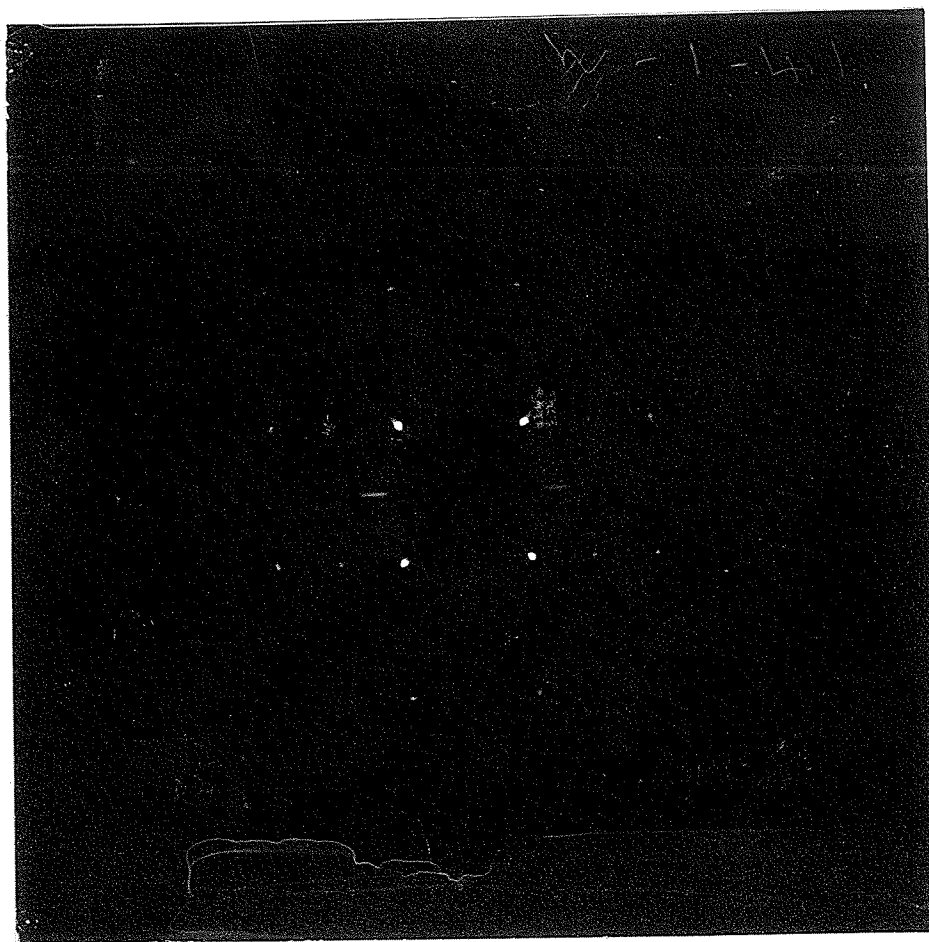
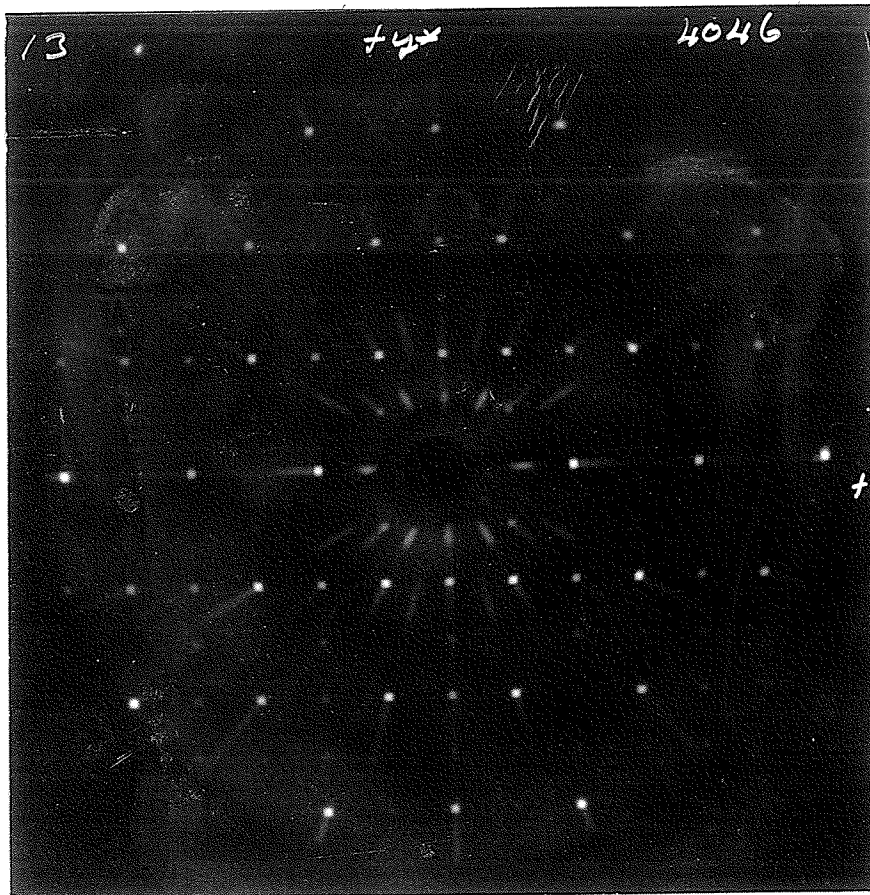


PLATE IIO-LEVEL INTEGRATED PRECESSIONPHOTOGRAPH ABOUT $x[100]$

Radiation Mo/Zn, $\bar{\mu} = 25^\circ$, $r_s = 15$ mm., $s = 32$ mm., $F = 60$ mm.,
rotation axis $z [001]$.



An attempt was made to record further upper levels using the non-integrating method but the precession camera proved so sensitive to orientation errors that the intensities of several pairs of symmetry-related reflections on these non-integrated photographs failed to give satisfactory agreement. Due to this, and the difficulty in scaling the intensities of the non-integrated reflections to the intensities of the integrated ones, the intensity data derived from the non-integrated films proved too unreliable to be used.

The integrated reflections which it was possible to record and which were used in the structure refinement, were those from the 0- and 1-level photographs precessing about the x axis and the 0-, 1- and 2-level photographs precessing about the y axis, i.e. the reflections $0kL$, $1kL$, $h1L$, and $h2L$. Cross-level photographs were also taken to obtain intensity values for reflections which fell in the blind areas of the previous photographs such as the $0l0$ reflection (see Plate Ia). However, for various reasons the data obtained from these cross-level photographs proved to be unsatisfactory and thus they were not used.

It is only possible to measure accurately the density of a spot (reflection) on a photograph within a limited range of density, as is more thoroughly explained in the next section. Thus, four photographs, of different exposure times, were taken of each reciprocal level. On the photograph with the shortest exposure time, the reflections with the strongest intensity were weak enough to be measured with reasonable accuracy, and on the photograph with the longest exposure time the weakest reflections appeared with a measurable density.

The exposure times were chosen so that the strongest and the weakest reflections on any given level could be measured on at least one

photograph of the set of four of that level. It was necessary to choose the exposure times as multiples of the integrating cycle of the camera, so that the spot on the photograph corresponding to a reflection had a uniform overall intensity. With the precession instrument used in this study, the time taken for one integrating cycle, i.e. for the cassette to be moved in horizontal and vertical steps of 0.08mm. over 1 square mm., is 1 hour and 20 minutes. The exposure times chosen were 2 cycles, 8 cycles, 13 cycles and 20 cycles.

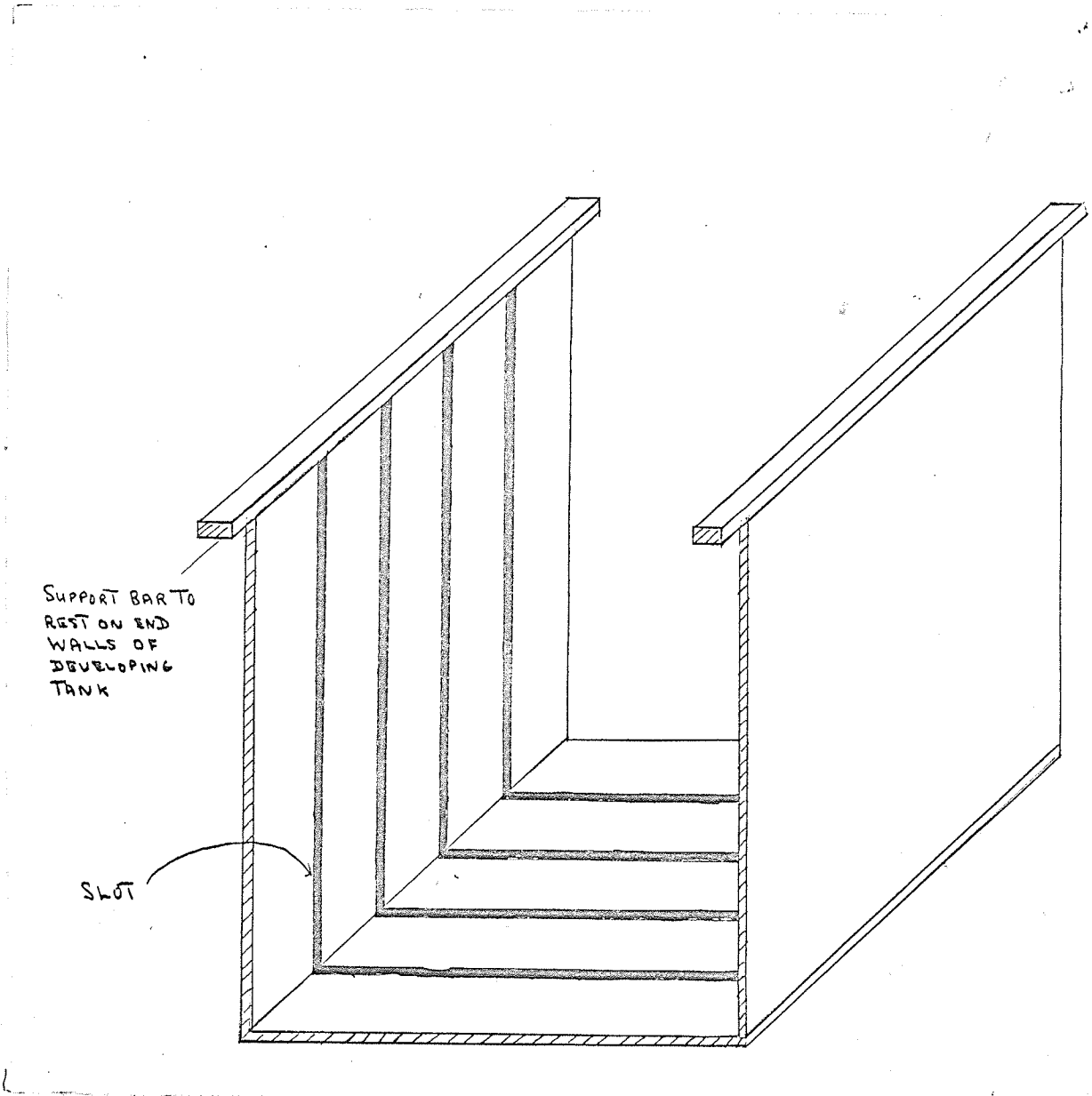
The density of spots on a photograph is also influenced by the length of the developing time and the strength of the developer. These were standardised by developing each set of photographs for a standard time in a solution of developer kept especially for this purpose. The four photographs of one level were mounted in an especially designed slotted plexiglas frame (see Fig. 2) that enabled them all to be submerged simultaneously in the developer and thus ensure the same developing time for each photograph in the set.

4) Density Measurement.

To measure the intensity of the reflections as they appeared on the photographs a densitometer (Universal) was used. The densitometer measures, by means of a photo-electric cell, the amount of incident light which is absorbed by the photograph at the point of measurement. It is only possible to measure the absorption at one point on the photograph at a time, and thus, the process of measurement is somewhat tedious by this method. One reading on each reflection was taken and one or two on the background for each reflection (see below).

Due to the nature of the developing process, it is only possible to preserve a linear relationship between exposure to X-rays and density

Figure 2. Apparatus used for simultaneously
developing four or five precession
photographs.



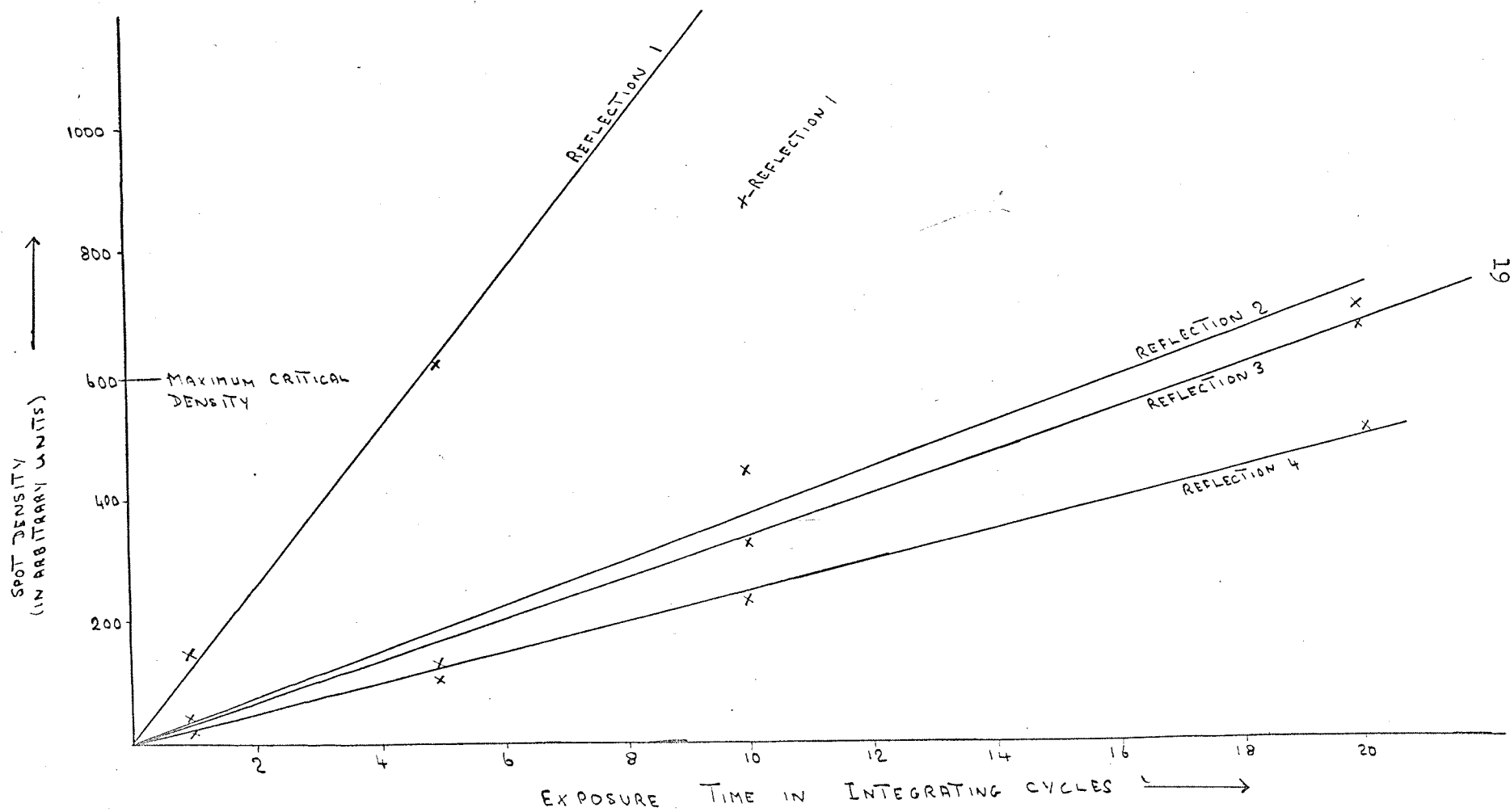
(or blackness) of a spot up to a certain maximum density. Therefore, values of density obtained above this maximum cannot be used in a straightforward manner as a measurement of the intensity of X-rays impinging on the film.

To determine this critical maximum value, a plot of density against exposure time was made for several different reflections. The plots are shown in Fig. 3. The reflections were chosen from a set of films, each of different exposure time, of one reciprocal lattice plane. As can be seen from Fig. 3, the linear relationship holds well for density values below 600; above this, however, the relationship becomes dubious, and densities measured above this value were not taken into account.

The intensity, I , of a reflection was determined by subtracting the density of the background darkening, D_s , from the density reading at the centre of the reflection, D_r . Where a white radiation streak through the reflection was visible, an average value of the densities of the streak on either side of the reflection was used for the background density value. Such I values were of course on an arbitrary scale.

The I values thus derived were used as input data for the first computer program, 'Precproc', for the first step in processing the data.

Figure 3. Plots of densities against exposure times for some wodginite reflections.



CHAPTER III
PROCESSING OF DATA

In order to obtain a set of observed structure factors from the raw intensity data, and to then find a crystal structure which was compatible with these structure factors, four computer programs were used. The first two of these, 'Precproc' and 'Dataps', originated at the Weizmann Institute in Israel, and were adapted for use with the I.B.M. 360/65 computer at the University of Manitoba, by Dr. W. Kaufman of the Department of Oral Biology, Faculty of Dentistry. The last two programs, 'Genles' and 'Fourier', are part of a set of structure programs written by Dr. Allen Larson of the United States Atomic Energy Commission, Los Alamos, New Mexico, and adapted to the I.B.M. 360/65 computer by Dr. Anne Kerr of the Department of Chemistry, University of Calgary.

A short description of each of these programs, together with the results obtained by their use in this structure analysis, follows.

1) 'Precproc' (Precession Processing)- Processing of Intensities from Precession Photographs to Give a Set of Relative Intensities.

'Precproc' is written especially for dealing with intensity data obtained from precession films. Its purpose is to produce a scaled and weighted intensity value for each reflection on a given reciprocal level from the various intensity values of that reflection derived from each of the differently exposed films of that level.

The program can deal with data from any number up to six differently exposed films of a given level at a time. It can be used to process a large number of levels in succession during one run. The card

input for this program as applied to wodginite is given in Appendix III.

The first aim of the program is to find one weighted and scaled value for each reflection from the four values obtained for that reflection from each of the differently exposed films for that level. Thus, on the OkL level for the 002 reflection, four intensity values: $I_1 = 745$, $I_2 = 395$, $I_3 = 320$ and $I_4 = 120$, corresponding to the intensity values on the four films of this level, are fed into the program as data. Each of these values is given a weight according to a predetermined weighting scheme:-

$$W = I, I \geq 15 \text{ and } I < 60,$$

$$W = 2I, I \geq 60 \text{ and } I < 200,$$

$$W = I/2, I \geq 200 \text{ and } I < \text{IMAX},$$

$$W = 0, I \geq \text{IMAX},$$

where W is the weight and IMAX is the maximum intensity reading up to which the linearity of the densitometer readings can be depended upon.

In this case $\text{IMAX} = 600$. Thus, $W_{I(1)} = 0$, $W_{I(2)} = 197$, $W_{I(3)} = 160$,

$$W_{I(4)} = 240.$$

From the whole set of reflection data for the OkL, average film-to-film ratios are computed, rejecting those individual ratios which are outside the range of twice the standard deviation from the mean. These film-to-film ratios for the OkL level were

$$r_{12} \text{ (ratio of 1st. film to 2nd. film)} = 1.52,$$

$$r_{23} = 1.29,$$

$$r_{34} = 4.00.$$

I_{scaled} , the scaled and weighted average intensity, for each reflection is then computed from the four original intensity values, assigned weights and film-to-film ratios, such that

$$I_{\text{scaled}} = \frac{I_1 W_{I(1)} + I_2 W_{I(2)} r_{12} + I_3 W_{I(3)} r_{12} r_{23} + I_4 W_{I(4)} r_{12} r_{23} r_{34}}{W_{I(1)} + W_{I(2)} + W_{I(3)} + W_{I(4)}}$$

Therefore, I_{scaled} for the 002 reflection is

$$\frac{745 + 395 \times 197 \times 1.52 + 320 \times 160 \times 1.52 \times 1.29 + 120 \times 240 \times 1.52 \times 1.29 \times 4.00}{0 + 197 + 160 + 240}$$

$$= 747.$$

The weight attached to this scaled intensity value is simply the sum of the weights assigned to I_1 , I_2 , I_3 , I_4 ,

$$\text{i.e. } W_{I(\text{sc } 002)} = 0 + 197 + 160 + 240 = 597.$$

The final function of the program is to average the scaled intensity values for symmetry related reflections. Thus, in this case the scaled intensity values for 002 and $00\bar{2}$ reflections are averaged to give a final intensity value I_{002} . The final weighting factor attached to this value is simply an average of those attached to $I_{\text{sc}(002)}$ and $I_{\text{sc}(00\bar{2})}$.

Thus the final output consists of a list of all the unique (non-symmetry related) reflections together with their intensity values and the weighting factor attached to this value by the program. For an example of the output from this program see Table IV. By this means, relative observed intensities for 190 reflections of wodginite were derived. These were put onto disk storage ready for input into 'Dataps', the next program.

2) 'Dataps' (Data Processing) - Data Reduction of the Relative Intensities to give a Set of Relative $|F_{\text{obs}}|$ Values.

This program is designed to make Lorentz, polarisation and absorption corrections to the observed relative intensities, and to thus, convert them into observed structure factors, F_{obs} 's:

$$(F_{\text{obs}})^2 = \frac{k \cdot I_{\text{obs}}}{\text{L.p}}$$

TABLE IVEXAMPLE OF OUTPUT DATA FROM PROGRAM 'PRECIFROC'FOR SPECIMEN REFLECTIONS FROM THE h11 LEVELREFLECTION DATA

H	K	L	FILM 1	FILM 2	FILM 3	FILM 4
1.	1.	-6.	30.	15.	0.	0.
1.	1.	-5.	190.	100.	45.	0.
1.	1.	-4.	80.	45.	10.	0.
1.	1.	-3.	505.	230.	110.	25.
1.	1.	-2.	260.	140.	50.	0.
1.	1.	-1.	620.	705.	602.	130.
1.	1.	1.	675.	785.	620.	152.
1.	1.	2.	280.	145.	45.	0.
1.	1.	3.	700.	325.	135.	25.
1.	1.	4.	100.	40.	0.	0.
1.	1.	5.	250.	120.	40.	0.
1.	1.	6.	80.	50.	0.	0.
-1.	1.	-6.	50.	25.	0.	0.
-1.	1.	-5.	205.	130.	60.	0.
-1.	1.	-4.	100.	50.	0.	0.
-1.	1.	-3.	605.	353.	120.	30.
-1.	1.	-2.	335.	180.	35.	0.
-1.	1.	-1.	-550.	-675.	-593.	-155.
-1.	1.	1.	640.	670.	600.	180.
-1.	1.	2.	375.	205.	40.	0.
-1.	1.	3.	685.	337.	140.	30.
-1.	1.	4.	140.	80.	0.	0.

Continued.

TABLE IV CONTD.

H	K	L	FILM 1	FILM 2	FILM 3	FILM 4
-1.	1.	5.	325.	160.	65.	0.
-1.	1.	6.	50.	200.	0.	0.

RATIO DATA BEFORE REJECTION

	I1/I2	I2/I3	I3/I4
FILM-TO-FILM RATIO	1.72	3.52	3.96
WEIGHTED FILM-TO-FILM RATIO	1.78	3.24	3.89
TOTAL NUMBER OF RATIOS	64	24	8
S.D (INDICATES ASSUMED INPUT VALUE)	0.35	0.98	0.81

RATIO DATA AFTER REJECTION

FILM-TO-FILM RATIO	1.74	3.26	3.75
WEIGHTED FILM-TO-FILM RATIO	1.78	3.10	3.71
TOTAL NUMBER OF RATIOS	64	24	8
S.D. (INDICATES ASSUMED INPUT VALUE)	0.24	0.84	0.62
NUMBER OF RATIOS WITHIN RANGE (2S.D.)	55	21	7

INTENSITY DATA

H	K	L	'I SCALED	WEIGHT	I1	I1/I2	I2	I2/I3	I3	I3/I4	I4
1.	1.	-6.	28.91	45.00	30.	2.00	15.	0.0	0.	0.0	0.
1.	1.	-5.	190.41	625.00	190.	1.90	100.	2.22	45.	0.0	0.
1.	1.	-4.	78.88	215.00	80.	1.78	45.	4.50	10.	0.0	0.
1.	1.	-3.	524.22	612.50	505.	2.20	230.	2.09	110.	4.40	25.
1.	1.	-2.	255.27	460.00	260.	1.86	140.	2.80	50.	0.0	0.
1.	1.	2.	263.74	475.00	280.	1.93	145.	3.22	45.	0.0	0.
1.	1.	3.	673.62	457.50	700.	0.0	325.	2.41	135.	5.40	25.
1.	1.	4.	95.21	240.00	100.	2.50	40.	0.0	0.	0.0	0.
1.	1.	5.	225.63	405.00	250.	2.08	120.	3.00	40.	0.0	0.
1.	1.	6.	82.16	210.00	80.	1.60	50.	0.0	0.	0.0	0.
-1.	1.	-6.	48.18	75.00	50.	2.00	25.	0.0	0.	0.0	0.
-1.	1.	-5.	250.73	482.50	205.	1.58	130.	2.17	60.	0.0	0.
-1.	1.	-4.	97.81	250.00	100.	2.00	50.	0.0	0.	0.0	0.
-1.	1.	-3.	646.06	446.50	605.	0.0	353.	2.94	120.	4.0	30.
-1.	1.	-2.	316.96	562.50	335.	1.86	180.	5.14	35.	0.0	0.
-1.	1.	2.	353.25	330.00	375.	1.83	205.	5.13	40.	0.0	0.
-1.	1.	3.	702.36	478.50	685.	0.0	337.	2.41	140.	4.67	30.
-1.	1.	4.	140.90	440.00	140.	1.75	80.	0.0	0.	0.0	0.

Continued.

TABLE IV CONTD.

H	K	L	I(H 1 L)	I(-H-1-L)	I(H-1 L)	I(-H 1-L)	I SCALED(MEAN)	WEIGHT
1.	1.	-4.	78.88	0.0	0.0	140.90	140.90	440.00
1.	1.	-3.	524.22	0.0	0.0	702.36	702.36	478.50
1.	1.	-2.	255.27	0.0	0.0	353.25	353.25	330.00
1.	1.	2.	263.74	0.0	0.0	316.96	316.96	562.50
1.	1.	3.	673.62	0.0	0.0	646.06	646.06	446.50
1.	1.	4.	95.21	0.0	0.0	97.81	97.81	250.00

NOTE: Ideally the program will calculate the mean of the two symmetry related intensity values and assign this mean value to the variable I SCALED(MEAN). However, because of the large discrepancy between the two symmetry related intensity values as shown above, the program was adjusted so that it selected the larger of these two values for I SCALED(MEAN).

where F_{obs} is the observed structure,
 I_{obs} is the observed intensity,
 L is the Lorentz factor,
 p is the polarisation factor,
 and k is a scale factor required to put the observed intensities on an absolute scale.

The program reads in all the intensity data stored on disk as output from 'Precproc' and all other supplementary information is read from cards. The card input as applied to wodginite is given in Appendix III.

An example of the printed output from 'Dataps' is illustrated in Table V. It lists for each reflection the hkl indices; I , the input intensity of the reflection; $I(\text{CORR})$, the intensity value corrected for absorption; ABS ('absorption') the transmission factor for X-rays for that hkl reflection; FOBS , the observed structure factor; WEIGHT , the weight assigned to that reflection; SINT , the $\sin\theta$ value of that reflection; and SCND , the index of the reciprocal level concerned (this increases by 1 for each additional level). The variables HKL , FOBS , WEIGHT and SINT are stored on disk for input into 'Genles', Larson's least squares program. It should be noted that because $F_{\text{obs}} \propto \sqrt{I_{\text{obs}}}$, it gives only the magnitude of F_{obs} and not the phase angle, and hence, it should more correctly be expressed as $|F_{\text{obs}}|$.

3) 'Genles' (General Least Squares)- Structure Factor Calculations and Refinement of Parameters by Least Squares.

The main input for this program consists of the reflection indices, $\sin\theta$, and F_{obs} for each of the reflections, together with a set of atomic parameters, anisotropic or isotropic temperature factors for

TABLE V

EXAMPLE OF OUTPUT DATA FROM PROGRAM 'DATAPS'

H	K	L	I	I(CORR)	SPOT	ABS	S(ABS)	F(OBS)	WEIGHT	SINT	SCND.
0.	6.	2.	675.81	67539.94	1.0000	0.0100	0.0	174.867	1.0000	0.39781	1
0.	6.	1.	38.40	4110.28	1.0000	0.0093	0.0	47.510	40.0000	0.37915	1
0.	6.	0.	431.87	47276.88	1.0000	0.0091	0.0	164.233	514.9995	0.37273	1
0.	5.	4.	63.33	5865.67	1.0000	0.0108	0.0	36.512	1.0000	0.41687	1
0.	5.	3.	28.45	3099.54	1.0000	0.0092	0.0	41.114	30.0000	0.37411	1
0.	5.	2.	36.42	4443.52	1.0000	0.0082	0.0	51.771	37.4999	0.34030	1
0.	5.	1.	31.40	4233.63	1.0000	0.0074	0.0	50.648	29.9999	0.31829	1
0.	5.	0.	28.45	3962.53	1.0000	0.0072	0.0	48.856	59.9998	0.31061	1
0.	4.	4.	69.94	7651.99	1.0000	0.0091	0.0	63.905	109.9999	0.37289	1
0.	4.	3.	384.04	50418.89	1.0000	0.0076	0.0	173.429	231.2498	0.32439	1
0.	4.	2.	63.32	9763.32	1.0000	0.0065	0.0	74.762	99.9998	0.28473	1
0.	4.	1.	562.41	95482.06	1.0000	0.0059	0.0	225.740	364.9983	0.25802	1
0.	4.	0.	215.16	38521.87	1.0000	0.0056	0.0	141.054	634.9990	0.24849	1
0.	3.	5.	10.00	1012.57	1.0000	0.0099	0.0	20.890	1.0000	0.39436	1
0.	3.	4.	57.39	7189.17	1.0000	0.0080	0.0	64.982	120.0001	0.33472	1
0.	3.	3.	10.00	1570.91	1.0000	0.0064	0.0	29.908	1.0000	0.27967	1
0.	3.	2.	83.20	16183.29	1.0000	0.0051	0.0	89.709	124.9994	0.23250	1

each atom, and atomic scattering curves for each atom type, in an assumed structure. A more detailed description of the input is given in Appendix III.

During one least squares cycle, both the magnitude and the phase angle of the structure factors, $\pm F_{\text{calc}}$, are calculated for the assumed structure from the given parameters and scattering curves. If the structure is centrosymmetric as is wadginitite, the phase angles will be either 0 or π radians, and the F_{calc} 's will be either +ve or -ve respectively; hence, the $\pm F_{\text{calc}}$. For each reflection $\Delta F = F_{\text{obs}} - F_{\text{calc}}$ is then calculated. It is usual to designate F_{obs} and F_{calc} as F_o and F_c respectively. The value of R, a measure of how close the assumed structure is to the actual structure is then calculated. In the form used here,

$$R = \frac{\sum(\Delta F)}{\sum F_o} \quad \text{over all reflections considered.}$$

By performing a least squares analysis, minimizing the function $\sum w_1 \left| |F_o| - |F_c| \right|^2$ where $w_1 = \frac{1}{\sigma^2 F_{\text{obs}}}$,

small adjustments are made to the original parameters so that a better agreement between the calculated and observed structure factors, i.e. the smallest value of the minimizing function, can be obtained. These new parameters are then fed into the next cycle when the whole process can be repeated.

The program can be made to perform as many cycles as is convenient. This is usually limited by computer time available for each run. It was found in this case that 3 cycles was a convenient number.

In theory, and if the assumed structure is essentially correct,

each successive cycle should give a better (lower) value for R, and the refinement can be continued in this way until an acceptable low R value is obtained. However, if the assumed structure is incorrect, unreasonably high R values will result, and the structure will not refine. In general, a mineral structure will likely not start to refine unless the initial R is less than perhaps 0.30.

The best value of R obtainable is determined by the accuracy of the data. Single-crystal diffractometer data can be expected to refine to an R of $\sim 0.30-0.05$, whereas photographic data cannot generally be expected to produce an R value better than 0.08-0.10 in a 3-dimensional refinement.

The 'Genles' program will print out, if it is desired, the following for each reflection: HKL, F_o , F_c and ΔF . As an example of the output, and as an important part of the results, the final least squares output for all reflections is shown in Tables VI and VIa below. In the programming sequence, the output from the program can also be stored on disk for input into the next program, 'Fourier'.

4) 'Fourier' - Calculation of F_o and ΔF Fourier Syntheses.

This program can be used to perform an F_o Fourier synthesis, a ΔF Fourier synthesis, or a Patterson synthesis. In this structure analysis it was used only for F_o and ΔF syntheses.

F_o Synthesis.

For the F_o synthesis the program will compute the electron density, ρ_o , at a series of specified points, X, Y, Z, in the unit cell, where

$$\rho_o(X,Y,Z) = \frac{1}{V} \sum_{hkl} F_o(h,k,l) e^{-i2\pi(hX+kY+lZ)}$$

TABLE VI
FINAL F_o'S AND F_c'S FOR ALL REFLECTIONS
 (AN EXAMPLE OF OUTPUT DATA
 FROM PROGRAM 'GENLES')

H	K	L	FOB	FCALC	H	K	L	FOB	FCALC	H	K	L	FOB	FCALC
0	6	2	92	-88	1	6	2	35	+34	1	3	-4	94	-101
0	6	1	25	+28	1	6	3	15	+12	1	3	-5	16	+11
0	6	0	86	+89	1	5	-4	53	+54	1	1	2	75	-73
0	5	4	19	-23	1	5	-3	64	-66	1	1	-6	32	-35
0	5	3	22	-23	1	5	-2	64	-69	1	1	-5	71	-84
0	5	2	27	+31	1	5	-1	89	+79	1	2	3	30	+32
0	5	1	27	+21	1	5	0	73	+72	1	2	5	17	-16
0	5	0	26	-31	1	5	1	82	-81	1	1	-3	120	+121
0	4	4	34	-28	1	5	2	69	-68	1	1	-4	58	+54
0	4	3	91	+96	1	5	3	70	+73	1	2	-4	21	+23
0	4	2	39	+34	1	5	4	50	+51	5	0	2	21	+21
0	4	1	119	-123	1	4	-5	25	-26	5	0	0	37	-34
0	4	0	74	-69	1	4	-3	32	+35	5	0	-2	38	+36
0	3	5	11	+7	1	4	-2	24	-20	4	0	4	69	+79
0	3	4	34	+28	1	4	-1	51	-44	4	0	2	100	-107
0	3	3	16	-10	1	4	0	16	+11	4	0	0	120	+138
0	3	2	47	-43	1	4	1	39	+36	4	0	-2	100	-105
0	3	1	16	+11	1	4	2	17	+7	3	0	4	49	-24
0	3	0	48	+48	1	4	3	34	-36	3	0	2	59	+55
0	2	5	77	+71	1	4	4	17	+13	3	0	0	40	-34
0	2	4	68	-63	1	4	5	29	+28	4	0	-4	97	+89
0	2	3	141	-128	1	1	3	118	-125	3	0	-2	31	+24
0	2	2	97	+89	1	1	4	58	+51	3	0	-4	45	-39
0	2	1	127	+119	1	1	5	86	+80	2	0	4	101	+114
0	2	0	96	-95	1	1	6	28	-35	2	0	2	137	-155
0	1	6	7	+10	1	2	1	79	-66	2	0	0	128	+130
0	1	5	24	-28	1	2	2	38	-31	2	0	-2	158	-168
0	1	4	21	-15	1	2	0	36	+32	2	0	-4	105	+115
0	1	3	38	+37	1	2	6	15	-15	1	0	4	53	-44
0	1	2	17	+20	1	2	4	18	+19	1	0	2	27	+12
0	1	1	15	-44	1	2	-1	21	+2	1	0	-2	98	+75
0	0	6	68	-81	1	2	-2	33	-25	1	0	-4	19	-22
0	0	4	101	+111	1	3	4	99	-96	1	0	-6	15	+25
0	0	2	142	-150	1	2	-3	31	-31	1	0	0	58	-59
1	7	-1	70	-77	1	2	-6	15	-15	5	1	3	75	-76
1	7	0	20	+19	1	3	5	16	-10	5	1	2	41	-44
1	7	1	70	+74	1	3	-1	16	+18	5	1	1	85	+81
1	6	-3	15	-13	1	3	1	17	-18	5	1	0	58	+51
1	6	-2	24	+29	1	3	2	121	+128	5	1	-1	92	-91
1	6	-1	23	+24	1	3	-2	114	+136	5	1	-2	37	-40
1	6	0	33	-34	1	3	0	141	-152	4	1	4	16	-11
1	6	1	16	-8	1	3	-3	17	-12	4	1	3	16	+25

Continued.

TABLE VI CONTD.

H	K	L	FOB	FCALC	H	K	L	FOB	FCALC	H	K	L	FOB	FCALC
4	1	2	16	+19	2	1	1	59	-46	4	2	-4	47	-50
4	1	1	30	-29	2	1	0	28	-23	3	2	5	30	-25
4	1	0	16	-10	2	1	-1	49	+35	3	2	4	16	+21
4	1	-1	45	+37	2	1	-2	36	+20	3	2	3	23	+22
4	1	-2	16	+13	2	1	-3	49	-35	3	2	2	20	-21
4	1	-3	16	-25	2	1	-5	34	+25	3	2	1	13	-17
4	1	-4	16	-14	1	1	-2	85	-72	3	2	0	27	+25
3	1	5	69	+69	5	1	-3	83	+79	3	2	-1	53	+48
3	1	2	66	-58	5	2	3	24	+23	3	2	-2	25	-26
3	1	1	138	+128	5	2	2	18	-21	3	2	-5	16	+16
3	1	4	55	+46	5	2	1	27	-30	3	2	-4	48	+19
3	1	3	100	-93	5	2	0	17	+20	3	2	-3	21	-23
3	1	-2	71	-66	5	2	-1	15	+15	2	2	5	79	+69
3	1	0	68	+60	5	2	-2	15	-17	2	2	4	57	-56
3	1	-1	140	-123	5	2	-3	21	-23	2	2	3	87	-82
3	1	-3	104	+101	4	2	4	47	-46	2	2	2	74	+74
3	1	-4	51	+46	4	2	3	91	-83	2	2	-2	72	+78
3	1	-5	74	-75	4	2	2	60	+60	2	2	-3	90	+85
2	1	5	30	-22	4	2	1	85	+82	2	2	-4	60	-58
2	1	4	18	-15	4	2	-1	90	-91	2	2	-5	84	-75
2	1	3	46	+35	4	2	-2	59	+61	0	0	0	248	+281
2	1	2	17	+12	4	2	-3	89	+89					

TABLE VIa

FINAL OUTPUT FROM 'GENLES' FOR LAST TWO LEAST SQUARES CYCLES

1WDDGINITE LEAST SQUARES												
OTHE JI ARE 4 0 0 1 1 1 3 0 0 3 0 0 0 1 1 0 1 0 40 -1												
OTHE FCRM FACTORS ARE												
OXYGEN	3.225630	18.499100	3.017170	6.656799	1.425529	0.405890	0.905250	61.188889	0.423620	0.0	0.0	0.0
TANT	28.175690	1.040339	14.428800	3.207840	12.641199	12.505400	3.744360	85.018295	13.982400	0.0	0.0	0.0
MANG	9.780939	4.983029	7.791530	0.304210	4.185439	11.439899	0.727360	27.774994	0.514540	0.0	0.0	0.0
LATTICE CONSTANTS ARE A # 4.7580 B # 5.7260 C # 5.1120 COSA # 0.00000 COSB # -0.01920 COSC # 0.00000												
OFORM FACTOR DESCRIPTION X Y Z B11 B22 B33 B12 B23 B31 P N FOLD												
X1-PC%<	<CP%<	<	0.29000	0.62000	0.08000	1.00000	0.0	0.0	0.0	0.0	0.0	4
X1-PC%<	<CP%<	<	0.24000	0.11000	0.07000	1.00000	0.0	0.0	0.0	0.0	0.0	4
X1-PC%<	<CP%<	<	0.50000	0.32500	0.25000	0.67800	0.0	0.0	0.0	0.0	0.0	2
X1-PC%<	<CP%<	<	0.0	0.82900	0.25000	0.61100	0.0	0.0	0.0	0.0	0.50000	2
OTHERS WERE 191 REFLECTIONS READ IN, OF WHICH 191 WERE OBSERVED												
OTHERS ARE 190 OBSERVED REFLECTIONS WITH SCALE 1												
OSCALE FACTORS ARE 1.90000												
OXYGEN	3.226	18.499	3.017	6.657	1.426	0.406	0.905	61.189	0.424	0.0	0.0	0.0
TANT	28.176	1.040	14.429	3.208	12.641	12.505	3.744	85.018	13.982	0.0	0.0	0.0
MANG	9.781	4.983	7.792	0.304	4.185	11.440	0.727	27.775	0.515	0.0	0.0	0.0
1WDDGINITE LEAST SQUARES												
- THE FOLLOWING ATOMS WERE MADE ANISOTROPIC												
O ATOM NAME NO. OLD B NEW B11JKS												
OXYGEN	1	1.00	0.011047	0.007625	0.009570	-0.000000	0.000395	-0.000000				
XYGEN	2	1.00	0.011047	0.007625	0.009570	-0.000000	0.000395	-0.000000				
TANT	3	0.68	0.007490	0.005170	0.006489	-0.000000	0.000268	-0.000000				
TANT	4	0.61	0.006750	0.004659	0.005847	-0.000000	0.000241	-0.000000				
1WDDGINITE LEAST SQUARES												
DATA SET												
THIS IS CYCLE NO. 1 IN THIS RUN. 190 REFLECTIONS WERE USED												
R # 0.1271 WEIGHTED R # 0.2178 SUMDELQ # 4.02694E 02 HAMILTONS R IS 0.2651 FOR DATA SET WITH SCALE 1												
THE GOODNESS OF FIT IS 1.58646												
STANDARD DEVIATION OF ELECTRON DENSITY IS 1.23CE OC												
O FORM FACTOR DESCRIP. NO. PARA. CHANGE STD. DEV. NEW VALUE DELTA/SIGMA												
SCALE 1 0.0 0.0 1.89599962 0.0 0												
O1-P% OXYGE<CP%< 1 X -0.00247630 0.01097642 0.28752363 2.2560E-01 1												
SET MULTIPLICITY IS 4 Y -0.00011701 0.01152898 0.61988288 1.0149E-02 2												
Z 0.00956830 0.00970118 0.68556826 9.8630E-01 3												
B11 0.01674147 0.02023855 0.02778864 8.2721E-01 4												
B22 0.00065187 0.01534566 0.00827683 4.2468E-02 5												
B33 0.02626489 0.01456816 0.03563503 1.8029E 00 6												
B12 0.02065695 0.04864252 0.02060568 4.2361E-01 7												
B13 -0.01047084 0.03015657 -0.01007609 3.4721E-01 8												
B23 0.03109919 0.02904933 0.03109918 1.0706E 00 9												
O1-P% OXYGE<CP%< 2 X 0.00588546 0.01130247 0.24588937 5.2108E-01 10												
SET MULTIPLICITY IS 4 Y 0.00160625 0.01187769 0.11160618 1.3523E-01 11												
Z 0.00994691 0.00885426 0.07954688 1.1234E 00 12												
B11 -0.01223144 0.02011041 0.0 6.0821E-01 13												
B22 0.01188506 0.01432992 0.01551001 8.0142E-01 14												
B33 0.02281090 0.01463761 0.03233104 1.5584E 00 15												
B12 0.00158615 0.04811569 0.0 3.2963E-02 16												
B13 0.02411275 0.03364621 0.0 7.1666E-01 17												
B23 -0.02676752 0.03052195 -0.02676752 8.7699E-01 18												
O1-P% TANT<CP%< 3 X 0.0 0.0 0.50000000 0.0 0												
SET MULTIPLICITY IS 2 Y 0.00027467 0.00071072 0.32527465 3.8646E-01 19												
Z 0.0 0.0 0.25000000 0.0 0												
B11 -0.00256757 0.00308370 0.00452241 9.6234E-01 20												
B22 -0.00155725 0.00208595 0.00361046 7.4607E-01 21												
B33 0.00247585 0.00238436 0.00896840 1.0401E 00 22												
B12 0.0 0.0 -0.00000000 0.0 0												
B13 0.00134217 0.00312134 0.00160981 4.3004E-01 23												
B23 0.0 0.0 -0.00000000 0.0 0												
P 0.09266853 0.04694673 0.09266853 1.9739E 00 24												
O1-P% TANT<CP%< 4 X 0.0 0.0 0.0 0.0 0												
SET MULTIPLICITY IS 2 Y 0.00119712 0.00139128 0.83019710 8.6044E-01 25												
Z 0.0 0.0 0.25000000 0.0 0												
B11 0.00059346 0.00605989 0.00774378 1.6402E-01 26												
B22 0.00584977 0.00414225 0.01050862 1.4122E 00 27												
B33 0.00353371 0.00469657 0.01243106 1.4018E 00 28												
B12 0.0 0.0 -0.00000000 0.0 0												
B13 0.00293101 0.00612522 0.00317220 4.7851E-01 29												
B23 0.0 0.0 -0.00000000 0.0 0												
P -0.02410647 0.04647706 0.47589350 5.1867E-01 30												
OXYGEN	3.226	18.499	3.017	6.657	1.426	0.406	0.905	61.189	0.424	0.0	0.0	0.0
TANT	28.176	1.040	14.429	3.208	12.641	12.505	3.744	85.018	13.982	0.0	0.0	0.0
MANG	9.781	4.983	7.792	0.304	4.185	11.440	0.727	27.775	0.515	0.0	0.0	0.0
1WDDGINITE LEAST SQUARES												
- THE FOLLOWING ATOMS WERE MADE ANISOTROPIC												
O ATOM NAME NO. OLD B NEW B11JKS												

TABLE VIa CONTD.

TWO-DIGIT LEAST SQUARES
DATA SET
THIS IS CYCLE NO. 2 IN THIS RUN. 190 REFLECTIONS WERE USED

R # 0.1051 WEIGHTED R # 0.1738 SUMDELTA # 2.47513E 02 HAMILTONS R IS 0.2078 FOR DATA SET WITH SCALE 1
THE GOODNESS OF FIT IS 1.24377

STANDARD DEVIATION OF ELECTRON DENSITY IS 9.850E-01
SCALE FACTOR DESCRIP. NO. PARA. CHANGE STD. DEV. NEW VALUE DELTA/SIGMA

SCALE	1							
01-P4 OXYGEN KSPZ	<	1	X	-0.00528633	0.01152035	1.89999952	0.0	0
SET MULTIPLICITY IS	4			0.00407297	0.01003250	0.26223729	4.5887E-01	1
			Z	0.0142493F	0.01057390	0.62395555	4.0595E-01	2
				0.00575231	0.02348571	0.10381758	1.3476E 00	3
			422	0.00629517	0.01338658	0.03754095	4.0829E-01	4
			333	0.01442943	0.02068393	0.01457199	4.7025E-01	5
			112	0.03293547	0.05166101	0.05026456	6.9764E-01	6
			313	-0.00204008	0.03877478	0.04677805	6.3753E-01	7
			423	0.04111369	0.03375186	-0.01211616	5.2614E-02	8
01-P4 OXYGEN KSPZ	<	2	X	0.00103521	0.00868361	0.05412801	1.2181E 00	9
SET MULTIPLICITY IS	4		Y	0.00305711	0.011748E2	0.24692917	1.1974E-01	10
			Z	-0.00266679	0.00956661	0.11466324	2.6027E-01	11
			111	-0.00305520	0.01412119	0.07728004	2.7876E-01	12
			322	0.01213203	0.01629011	0.0	2.1903E-01	13
			433	-0.00351500	0.01895361	0.03164204	7.4521E-01	14
			112	-0.00005685	0.03767405	0.02888524	1.8549E-01	15
			313	0.01560465	0.02846767	0.0	5.3344E-01	16
			423	-0.05428580	0.03607261	-0.06044352	5.4815E-01	17
01-P4 TANT KSPZ	<	3	X	0.0	0.0	0.50000000	1.5049E 00	18
SET MULTIPLICITY IS	2		Y	-0.00019015	0.00060517	0.32508445	0.0	0
			Z	0.0	0.0	0.25000000	3.1422E-01	19
			111	0.00044703	0.00258800	0.00496944	0.0	0
			322	0.00020140	0.00176592	0.00381186	1.7273E-01	20
			433	0.00093415	0.00210049	0.00990655	1.1405E-01	21
			112	0.0	0.0	-0.00000000	4.4664E-01	22
			313	0.00009242	0.00267070	0.00170273	0.0	0
			423	0.0	0.0	-0.00000000	3.4793E-02	23
			P	-0.01025261	0.03698531	0.08247588	0.0	0
01-P4 TANT KSPZ	<	4	X	0.0	0.0	0.0	2.7721E-01	24
SET MULTIPLICITY IS	2		Y	-0.00005647	0.00120562	0.83014059	0.0	0
			Z	0.0	0.0	0.25000000	4.6845E-02	25
			111	0.00103327	0.00483558	0.00877704	0.0	0
			322	0.00077727	0.00361902	0.01128588	2.1368E-01	26
			433	0.00093653	0.00402047	0.01336959	2.1477E-01	27
			112	0.0	0.0	-0.00000000	2.3344E-01	28
			313	0.00081966	0.00511227	0.00399186	0.0	0
			423	0.0	0.0	-0.00000000	1.6033E-01	29
			P	-0.01750080	0.03851663	0.46839267	0.0	0
							1.9473E-01	30

in which V is the volume of the unit cell.

$F_o(h,k,l)$ is the observed structure factor for the (h,k,l) reflection given the phase (+ or -) in the centrosymmetric case like wadginite of the corresponding calculated structure factor obtained from the assumed structure used in the least squares analysis. The input to the program consists of the output tape from 'Genles' together with the necessary grid specifications on cards. For fuller details see Appendix III.

The results appear in the output as a series of two-dimensional grid sections. It is possible to have either X, Y- sections printed out in steps along the Z-axis; X,Z- sections along the Y-axis or Y,Z- sections along the X-axis, and it is also possible to designate which axis is to be horizontal and which vertical in the printout of the sections. It is also possible to specify the intervals desired between the grid points along all 3 axes independently, and so to specify the maximum and minimum limits along the X,Y,Z directions. For examples of the printed output see the next Chapter.

The F_o maps will, of course, show peaks where atoms were assumed to be located in the assumed structure, but it will also tend to show peaks where there are atoms in the real structure not postulated for the assumed structure. Thus, the need to make some slight change in an assumed atomic position may be indicated by the electron density peak being offset from the assumed position. If the needed change in position of one atom is quite large, a new peak may appear on the map which does not correspond to any atom in the assumed structure.

While this is a fairly good method of determining the positions of the heavier metal atoms in a structure (tantalum and manganese in

the case of wadginite), the peaks which correspond to the lighter oxygen atoms become overshadowed by the metal atom peaks and are thus virtually invisible.

In order to distinguish the oxygen positions more clearly, the more sensitive difference map must be used.

ΔF Synthesis

The program works in exactly the same way for the ΔF synthesis as for the F_o synthesis except that instead of the terms in the Fourier series being F_o , they are $F_o - F_c$, and hence, the result is a map not of the observed electron densities at a point X,Y,Z, but of $\rho_o - \rho_c$, the difference between the observed and calculated electron densities at a point X, Y, Z.

Thus, where there is agreement between the actual structure (F_o) and the assumed structure (F_c) the difference map will ideally be flat; where there is an atom in the actual structure which was not assumed to be in the assumed structure, there will be a positive peak; and where there is an atom in the assumed structure which is not in the actual structure, there will be a negative peak.

Therefore, once the heavy atom positions have been found by an F_o synthesis, the difference synthesis provides a valuable way of determining the positions of the lighter atoms.

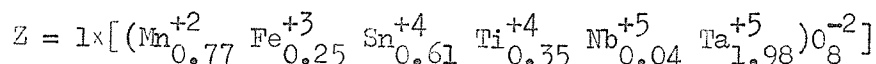
CHAPTER IV

THE STRUCTURE ANALYSIS1) The Starting Structure from that of Columbite-Tantalite.

It was explained in Chapter I that only the small sub-cell of wodginite was used for this structure analysis due to the weakness of reflections marking the larger true cell. In Chapter II it was shown that the sub-cell has the dimensions

$$\underline{a} = 4.758 \text{ \AA}, \underline{b} = 5.726 \text{ \AA}, \underline{c} = 5.112 \text{ \AA}, \beta = 91^{\circ}08'$$

and in Chapter I it was shown that the sub-cell has the content



which is one quarter the content of the large cell. The space group of this small cell was found (Chapter I) to be P2/c (centrosymmetric) or Pc (non-centrosymmetric). Because the starting structure columbite-tantalite is centrosymmetric, the structure of wodginite was assumed to be also centrosymmetric and hence, to have space group P2/c. The assumption proved subsequently to be correct.

It was shown earlier that there is strong evidence that wodginite almost certainly has essentially the same structure as tantalite-columbite. Thus, the obvious starting structure for wodginite should be one derived from the structure of columbite by Sturdivant (1930). Since columbite-tantalite is an isostructural series and since wodginite is Ta-rich as is tantalite, Sturdivant's structure is from here on referred to as the structure of tantalite in this thesis.

Table II shows that the unit cell of tantalite contains $A_4 B_8 O_{24}$ where A = Mn, Fe, Sn, Ti, etc. and B = Ta and Nb. If one does not differentiate the A and B type atoms, then the cell content of tantalite could alternatively be written as $(A,B)_{12} O_{24}$ (which is a more useful

form for comparison with wodginite). Table II also shows that the content for the sub-cell of wodginite (used for the analysis) is $A_2B_2O_8$, or again not differentiating the A and B atoms, $(A,B)_4O_8$ which is the preferable form of writing the content of wodginite because at the start it was not known whether there was any ordering or differentiating of the metal atoms into the two structural sites. Thus, there are one third the number of atoms in the wodginite cell that there are in the tantalite cell, and consequently it is necessary to choose one third of the tantalite structure to represent the possible wodginite structure.

Table II also shows that the reason the wodginite cell has one third the volume of the tantalite cell is because $a_{\text{wodg}} \sim 1/3 a_{\text{tant}}$ whereas the b and c dimensions are approximately the same. Thus, the starting structure for wodginite had to be one with the same b and c periods, but one third the a period, of tantalite. Fig. 1a a projection of the tantalite structure along the y-axis, shows the structure extended along x, and it is one third of this a repeat of the tantalite structure that had to be chosen for the wodginite structure. It can also be seen from Fig. 1a that the tantalite structure has a pseudo repeat period of $a/3$ and this ties the wodginite structure even closer to it.

The following are the possible equivalent positions in the space group $P2/c$ (number 13 in the International Tables for X-ray Crystallography, Vol. I):

<u>No. of</u> <u>equipoints</u>	<u>Symbol</u>	<u>Parameters</u>
4	g	$x, y, z; \bar{x}, \bar{y}, \bar{z}; \bar{x}, y, \frac{1}{2}-z; x, \bar{y},$
2	f	$\frac{1}{2}, y, \frac{1}{4}; \frac{1}{2}, \bar{y}, \frac{3}{4}. \quad \frac{1}{2}+z.$
2	e	$0, y, \frac{1}{4}; 0, \bar{y}, \frac{3}{4}.$
2	d	$\frac{1}{2}, 0, 0; \frac{1}{2}, 0, \frac{1}{2}.$
2	c	$0, \frac{1}{2}, 0; 0, \frac{1}{2}, \frac{1}{2}.$
2	b	$\frac{1}{2}, \frac{1}{2}, 0; \frac{1}{2}, \frac{1}{2}, \frac{1}{2}.$
2	a	$0, 0, 0; 0, 0, \frac{1}{2}.$

Examination of the structure of tantalite in Fig. 1a, shows that there are 2-fold axes parallel to \underline{y} through the Mn position, that is, through every third metal atom site parallel to \underline{x} . However, the Fig. also shows that through the other metal atom sites (Ta), there are pseudo-2-fold axes. In a structure such as wodginite that is very close to that of tantalite and having space group symmetry $\underline{P2/c}$, there would have to be 2-fold axes parallel to \underline{y} through every metal site (Fig. 1b). Thus, when choosing a possible wodginite structure it is necessary to choose an origin (for wodginite) at either point A or point B in Fig. 1a. Either origin places all the metal atoms of wodginite on 2-fold axes, and hence, in the two 2-fold equivalent sites (e) $0, y, 1/4$ and (f) $1/2, y, 1/4$.

This division of the metal atoms into 2-fold sites makes it crystallographically possible to have segregation or ordering of the metals into two sites. This crystallographic possibility is itself not evidence that the structure will be ordered with respect to metal atoms. However, the chemical analysis of this wodginite (described earlier) shows that it contains ~ 2 Ta atoms per cell and ~ 2 of all the other

metals per cell, and so the chemistry suggests that the Ta atoms may be ordered into one site and all the other metal atoms into the other. On the other hand, all four metal atoms may, despite the chemistry, be disordered amongst the two 2-fold sites, and in fact this distribution of the metal atoms was assumed for the starting structure, Model I, so as not to bias the metal atom distribution into the two sites.

There appeared to be no particular reason to choose one origin in preference to the other, and so origin B was arbitrarily chosen. The two metal sites were designated M_1 and M_2 , and the two 4-fold general oxygen sites were designated O_1 and O_2 . From all these considerations and from the parameters given by Sturdivant (1930) for his atoms, the following parameters were assigned to the atoms in the starting structure, Model I, of wodginite.

M_1 2(disordered) metals in f $1/2, y, 1/4$ with $y = 0.325$.

M_2 2(disordered) metals in e $0, y, 1/4$ with $y = 0.825$.

O_1 4 oxygens in g x, y, z with $x = 0.25, y = 0.58, z = 0.43$.

O_2 4 oxygens in g x, y, z with $x = 0.25, y = 0.08, z = 0.43$.

2) Solution of the Structure.

Once the starting structure had been decided upon, the intensity data were processed by computer programs 'Frecproc' and 'Dataps' as described above. In the 'Dataps' program, scale factors for the intensities from the different precession levels were assigned in order to put the intensities from all levels on the same scale for input into the least squares program, 'Genles'. These scale factors were determined according to initial film exposure time, and were:-

OkL-level Scale factor = 1.0.

IkL-level Scale factor = 1.0.

h0L-level Scale factor = 1.0.

h1L-level Scale factor = 0.90.

h2L-level Scale factor = 0.95.

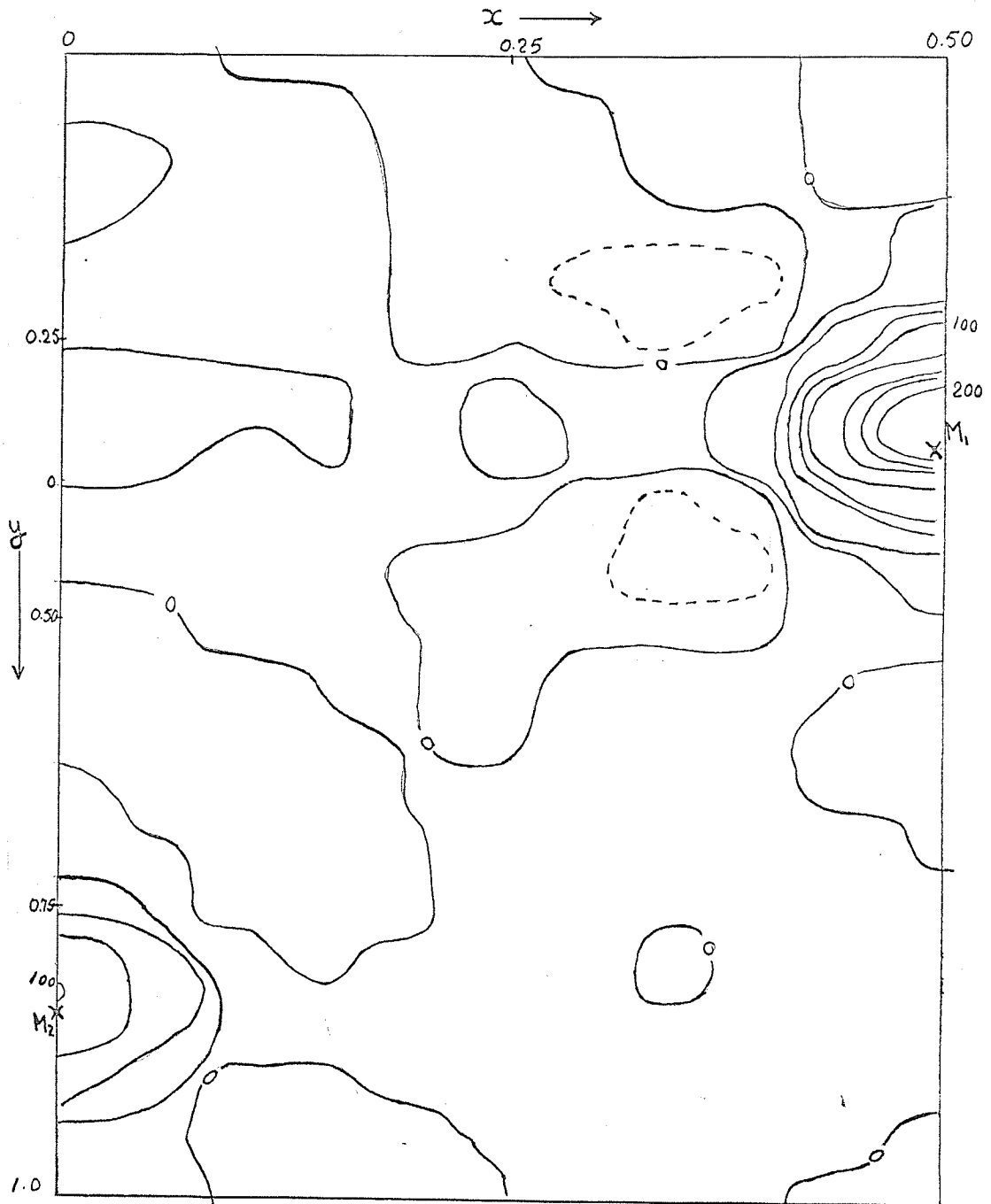
The output from 'Datans' was then run as input in 'Genles' using structure model I as the assumed structure and assuming a disordered distribution of the metal atoms. Metal atom disorder was taken account of by giving both the M_1 and M_2 sites or ''atoms'' effective scattering factors equal to one half the electrons in Ta^{+5} plus one half those in the ''mixed atom'' composed of proportional parts of Mn^{+2} , Sn^{+4} , Ti^{+4} , Fe^{+2} and Nb^{+5} according to the chemical composition (Chapter I, Section (3)). The scattering values used for the ''mixed atom'' were calculated as a weighted average of the scattering values listed for its component atoms, the weights being the proportion of the individual atoms contributing towards the ''mixed atom''.

A few runs using 'Genles' showed that the structure model was reasonably close to the real structure. Some difficulty was experienced refining the scale factor, k , where $F_o = kF_c$, but a value of 1.9 was eventually found to be satisfactory. Further refinement of the various scale factors is discussed below.

Using this scale factor, $k = 1.9$, and allowing the occupancy factors to vary, the best agreement between F_o 's and F_c 's yielded an R factor ($=100\Delta F/\Sigma F_o$) of $\sim 16\%$, and was given by a metal-ordered arrangement of Model I with the two Ta atoms in site M_1 and the two ''mixed atoms'' in site M_2 . F_o and ΔF syntheses were computed using program 'Fourier' and sections of the resulting maps are reproduced as Figs. 4 and 5.

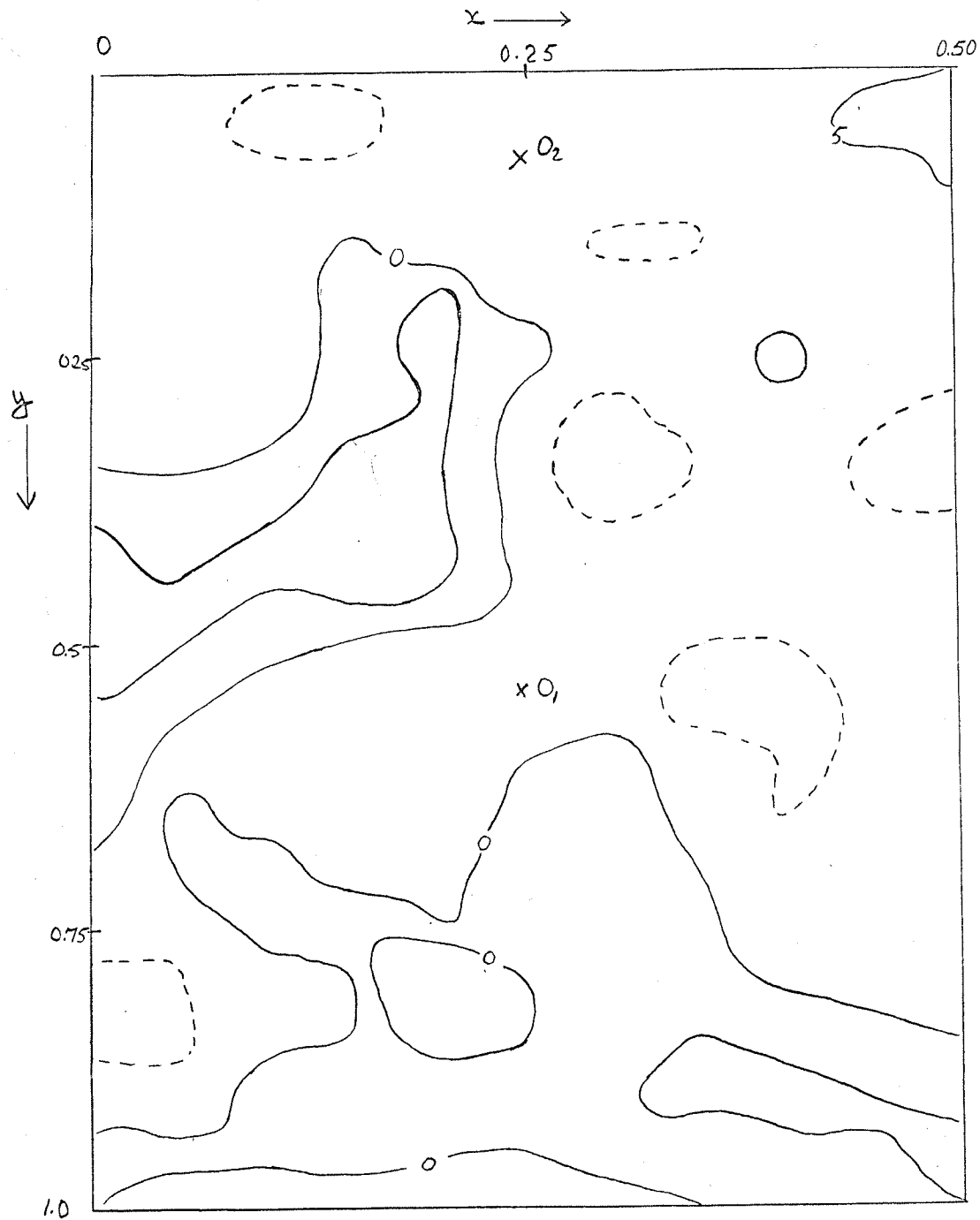
As can be seen from Fig. 4a, the electron density section at $z = 0.25$

Figure 4a. Electron density map (F_0 Synthesis) from Model I. x y section at $z = 0.25$. Contour interval $25\text{e}\text{\AA}^{-3}$.

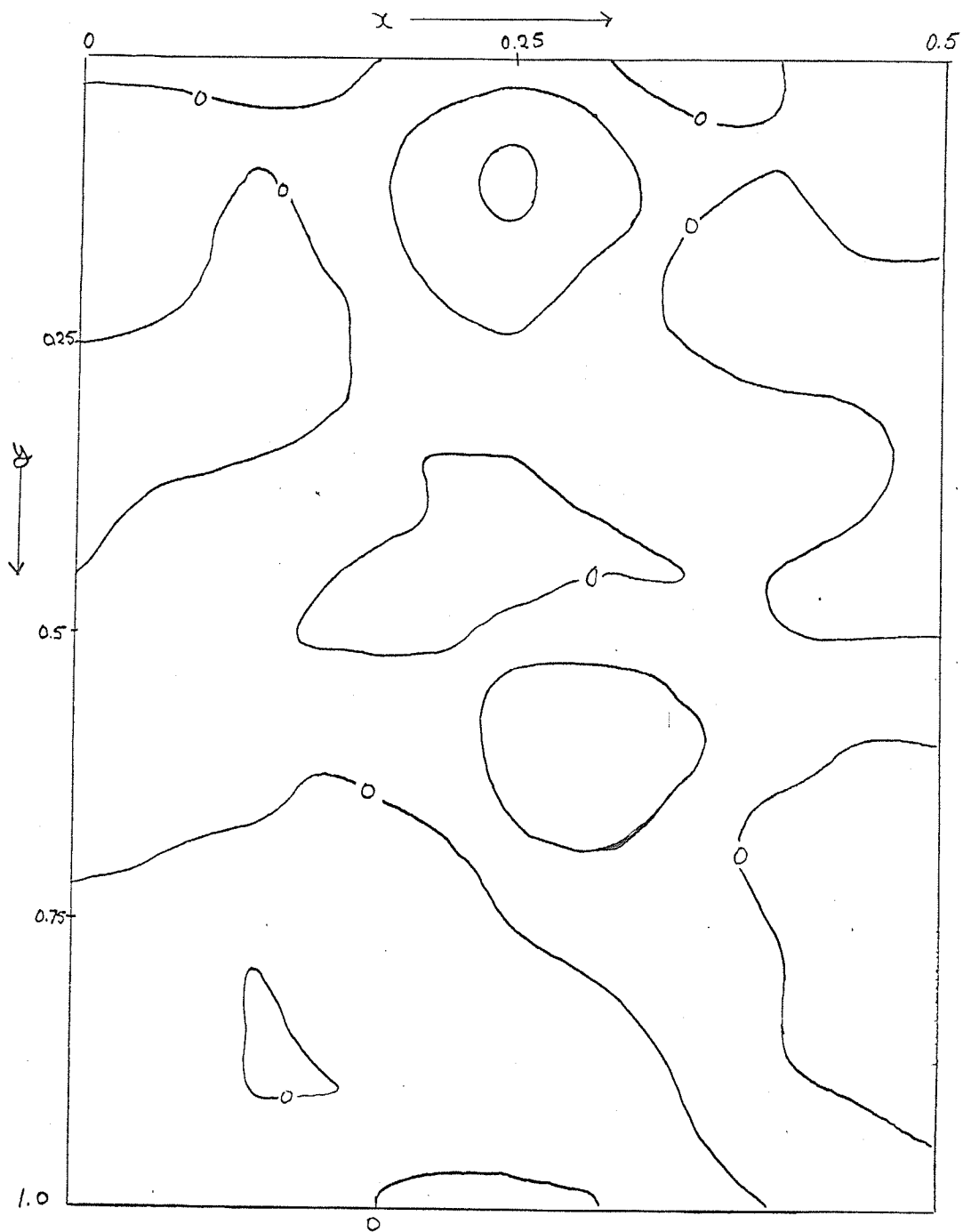


Assumed positions denoted by crosses. Zero and positive contours are solid lines, negative contours are dashed lines.

Figure 4b. Electron density map (F_0 Synthesis) from Model I. x y section at $z = 0.45$. Contour interval $5e^8 \text{Å}^{-3}$.



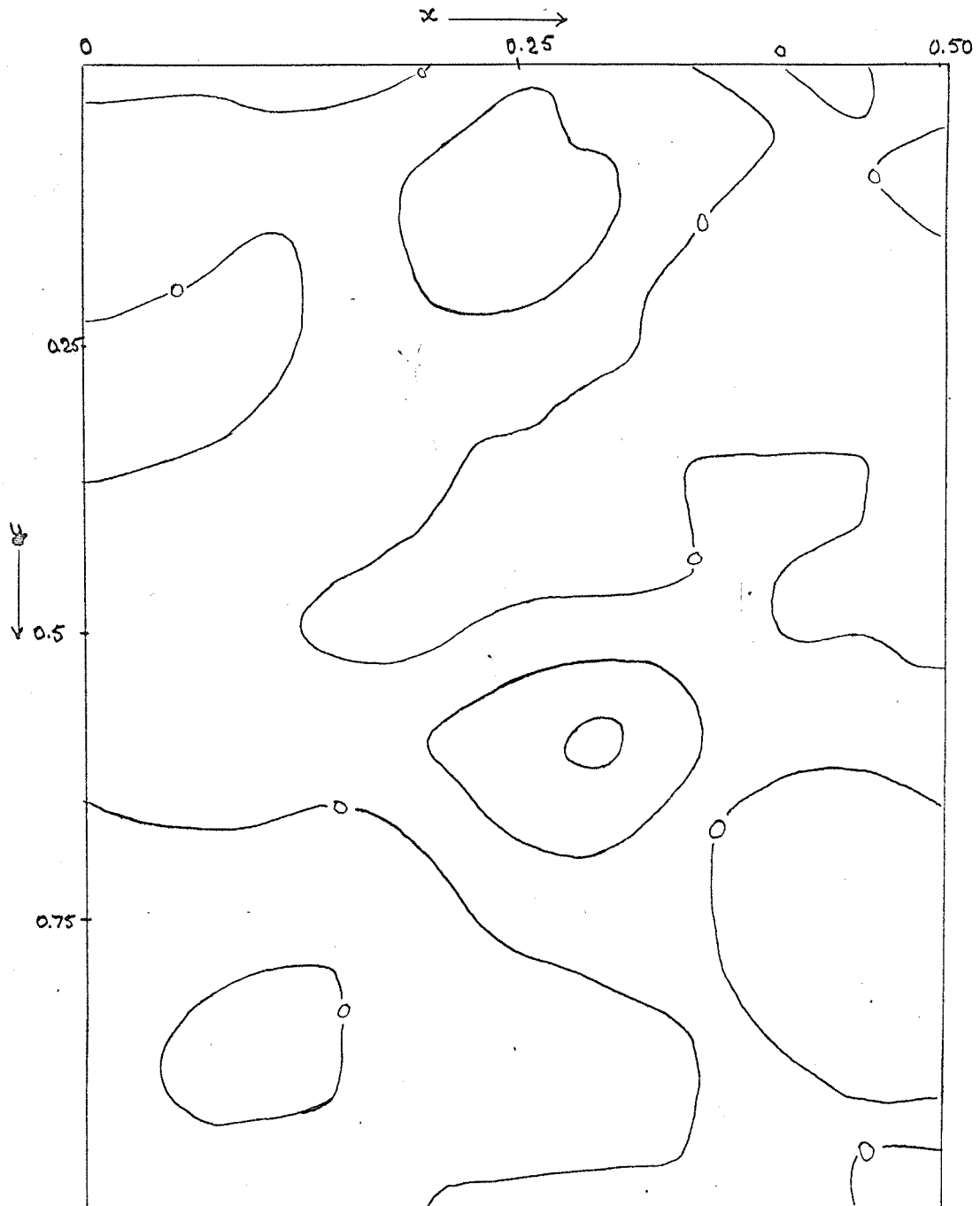
Assumed positions denoted by crosses. Zero and positive contours are solid lines; negative contours are dashed lines.

Figure 5a. Difference map (ΔF Synthesis) from Model I.

x y section at $z = 0.10$. Contour interval $5e^{\circ-3}$.

Assumed positions denoted by crosses. Zero and positive contours are solid lines, negative contours are dashed line.

Figure 5b. Difference map (ΔF Synthesis) from Model I.
x y section at $z = 0.05$. Contour interval $5e\text{\AA}^{-3}$.



Assumed positions denoted by crosses. Zero and positive contours are solid lines, negative contours are dashed lines.

confirms the positions of Ta^{+5} (with 68 electrons) in site M_1 at $x = 1/2$, $y = 0.325$ and $z = 1/4$, and of the 'mixed atom' in site M_2 at $x = 0$, $y = 0.825$ and $z = 1/4$. (The effective number of electrons of the 'mixed atom' will be, from the formula given in Chapter I, section (3),

$$\begin{aligned} & 1/2(0.77 Mn^{+2} + 0.25 Fe^{+2} + 0.61 Sn^{+4} + 0.35 Ti^{+4} + 0.04 Nb^{+5}) \\ &= 1/2 (0.77 \times 23 + 0.25 \times 24 + 0.61 \times 50 + 0.35 \times 22 + 0.04 \times 41) \\ &= 1/2(63.5) \\ &= 31.75 \text{ electrons.} \end{aligned}$$

No other peaks of any significance occur anywhere else on the map and the positions of the peaks on this section at $z = 0.25$ suggest that the best positional parameters for the metal atoms are not significantly different from those originally assumed.

Examination of the ρ_o section at $z = 0.45$ (Fig. 4b) shows no definite sign of the oxygen atoms which were assumed to be present in the positions shown near this section. However, examination of the $\rho_o - \rho_c$ sections at $z = 0.10$ and $z = 0.05$ (Figs. 5a and 5b, respectively), reveals small peaks at approximately $x = 0.25$, $y = 0.10$ and $z = 0.10$ and also at approximately $x = 0.30$, $y = 0.60$ and $z = 0.05$. This suggests a change in positions of the two oxygen atoms to these new locations. These new locations are, like the original oxygen sites, in general positions in the space group. Thus a new modified structure was formulated, Model II, with the metal atoms in the same positions as in Model I but now Ta-ordered, and with the oxygens in the new sites. The parameters used for Model II were as follows:

- M_1 2 tantalums in f $1/2, y, 1/4$ with $y = 0.325$
- M_2 2 'mixed atoms' in e $0, y, 1/4$ with $y = 0.825$
- O_1 4 oxygens in g x, y, z with $x = 0.30, y = 0.60, z = 0.05$

O_2 4 oxygens in g x, y, z with $x = 0.25$, $y = 0.10$, $z = 0.10$

When this structure was put through the least squares program, an R factor of $\sim 12\%$ was obtained.

It has been briefly noted earlier in this section that refining of the scale factor, k , had caused some difficulty; in addition to this, the overall scale factors, k_i , used for scaling each reciprocal level in 'Dataps' and derived from exposure times, were only approximations. Therefore, in order to refine the scale factors level by level, a new value, K_i , was calculated for each reciprocal level from the values of F_o and F_c which had given the best value for R ($\sim 12\%$), where

$$K_i = \frac{\sum F_o}{\sum F_c} \quad \text{over all reflections on the } i\text{th reciprocal level.}$$

Thus, a new scale factor, k_i' , was obtained for each level for re-input into 'Dataps', where $k_i' = k_i K_i$.

The new set of scale factors were:-

OkL-level Scale factor $k' = 1.0886$

lkL-level Scale factor $k' = 0.9334$

hOL-level Scale factor $k' = 0.9725$

hll-level Scale factor $k' = 0.7152$

h2L-level Scale factor $k' = 0.9278$

These scale factors were fed into 'Dataps' and all the data re-processed; and finally structure, Model II, was refined using the least squares program. This procedure resulted in a final R factor of 10.5%, and since there were no appreciable changes in either the positional, temperature or scale factors in the last two or three cycles of least squares refinement, the structure was regarded as being refined to the

limits of the intensity data used. The final positional and anisotropic temperature factors are given in Table VII. Final ρ_o and $\rho_o - \rho_c$ sections are shown in Figs. 6a, b and c and 7a and b.

The final structure is illustrated in Fig. 8. If Fig. 8 is compared with the projection of the tantalite structure in Fig. 1a and that of Model I of wodginite in Fig. 1b, it can be seen that apart from the oxygens, the final structure is **reasonably** close to the wodginite structure that would arise if one chose origin A in Fig. 1a. The oxygen atoms in the final structure appear to be in quite different positions relative to the metal atoms than are any oxygens in the tantalite structure in Fig. 1a.

The bond lengths are given in Table VIII, and the interbond angles in Table IX. The metal-oxygen bond lengths are also shown in Fig. 8 which shows that both the Ta atom and the 'mixed atom' (site M_2) are pseudo-octahedrally coordinated by oxygen atoms.

TABLE VII
FINAL ATOMIC PARAMETERS

<u>Site</u>	<u>Multi-</u>	<u>Atom(s)</u>	<u>Site</u>	<u>Site</u>	<u>Parameters and S.D.*.</u>		
<u>Symbol</u>	<u>plicity</u>		<u>Letter</u>	<u>Parameters</u>	<u>x</u>	<u>y</u>	<u>z</u>
M ₁	2	Ta	f	1/2,y,1/4	1/2	0.325(0.001)	1/4
M ₂	2	'mix met'***	e	0, y, 1/4	0	0.830(0.001)	1/4
O ₁	4	Oxygen 1	g	x, y, z	0.282(0.012)	0.624(0.010)	0.104(0.011)
O ₂	4	Oxygen 2	g	x, y, z	0.247(0.009)	0.115(0.012)	0.078(0.010)

* S.D. = Standard Deviation

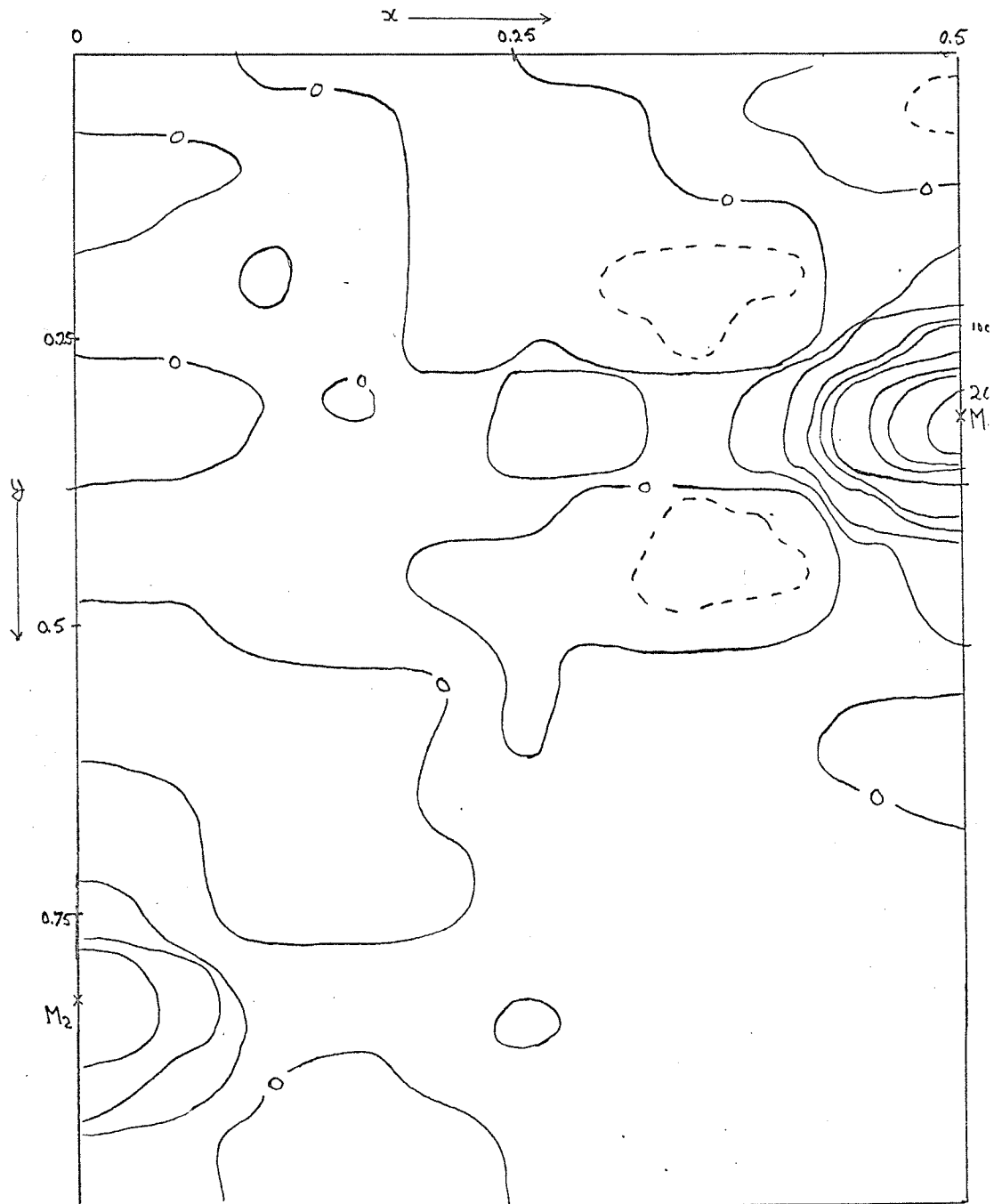
** 'Mix met' = 'Mixed metal atom' with composition from chemical analysis in atomic percentages of 38.3 Mn, 29.8 Sn, 14.4 Ti, 12.3 Fe, 2.2 Nb (Total 100.0%)(Chapter I, Section (3)).

TABLE VII CONTD.

<u>Site</u>	<u>Temperature Factors β_{ij} and S.D.*</u>
<u>Symbol</u>	
M_1	$\beta_{11} = 0.005(0.003), \beta_{22} = 0.004(0.002)$ $\beta_{33} = 0.010(0.002), \beta_{12} = -0.000(0.000)$ $\beta_{13} = 0.002(0.003), \beta_{23} = -0.000(0.000)$
M_2	$\beta_{11} = 0.009(0.005), \beta_{22} = 0.011(0.004)$ $\beta_{33} = 0.013(0.004), \beta_{12} = -0.000(0.000)$ $\beta_{13} = 0.004(0.005), \beta_{23} = -0.000(0.000)$
O_1	$\beta_{11} = 0.038(0.024), \beta_{22} = 0.015(0.013)$ $\beta_{33} = 0.050(0.021), \beta_{12} = 0.047(0.052)$ $\beta_{13} = 0.012(0.039), \beta_{23} = 0.054(0.034)$
O_2	$\beta_{11} = 0.000(0.000), \beta_{22} = 0.032(0.016)$ $\beta_{33} = 0.029(0.019), \beta_{12} = 0.000(0.000)$ $\beta_{13} = 0.000(0.000), \beta_{23} = -0.060(0.036)$

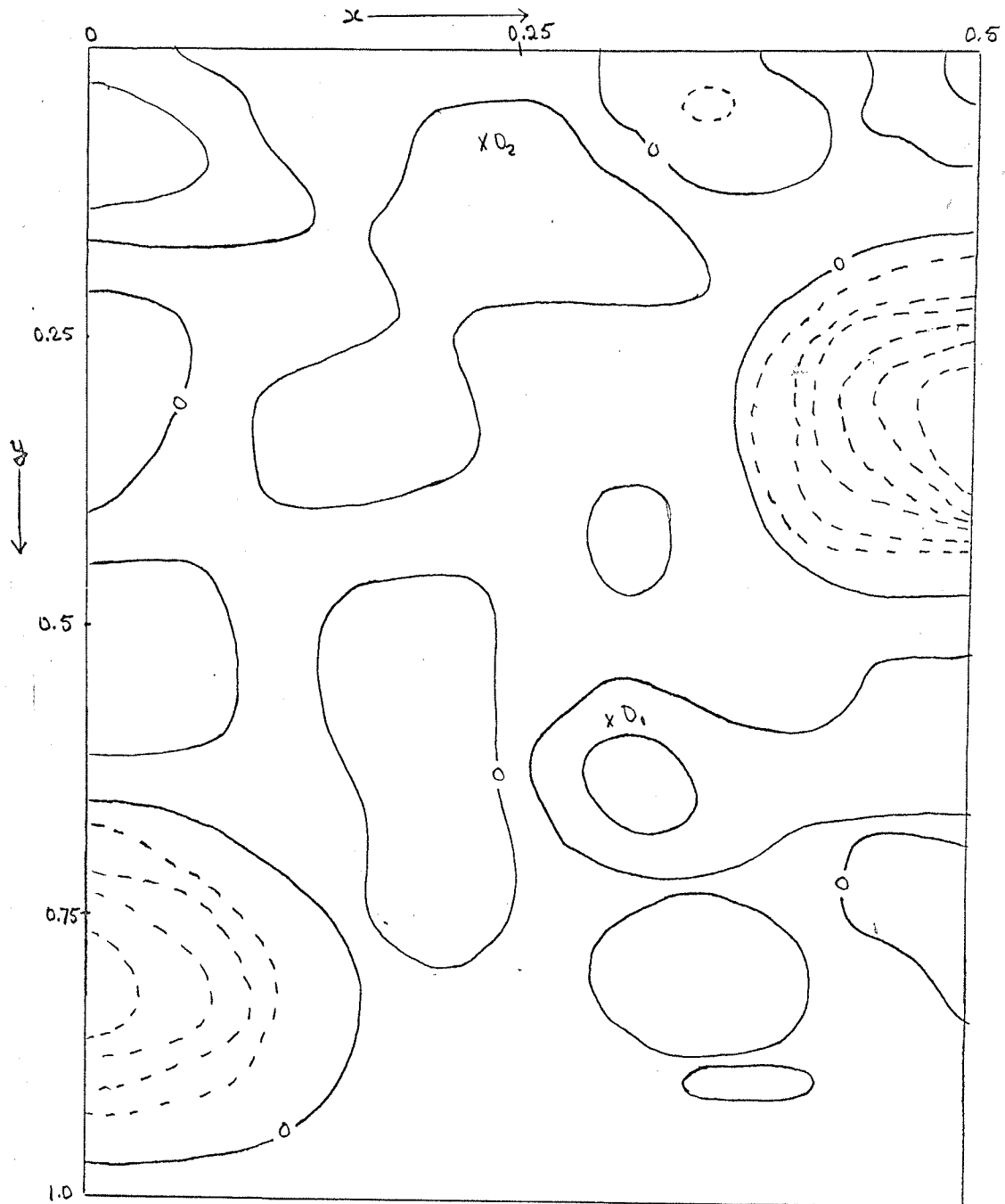
*S.D = Standard Deviation

Figure 6a. Electron density map (F_0 Synthesis) from final structure. x y section at $z = 0.25$. Contour interval $25eA^{-3}$.



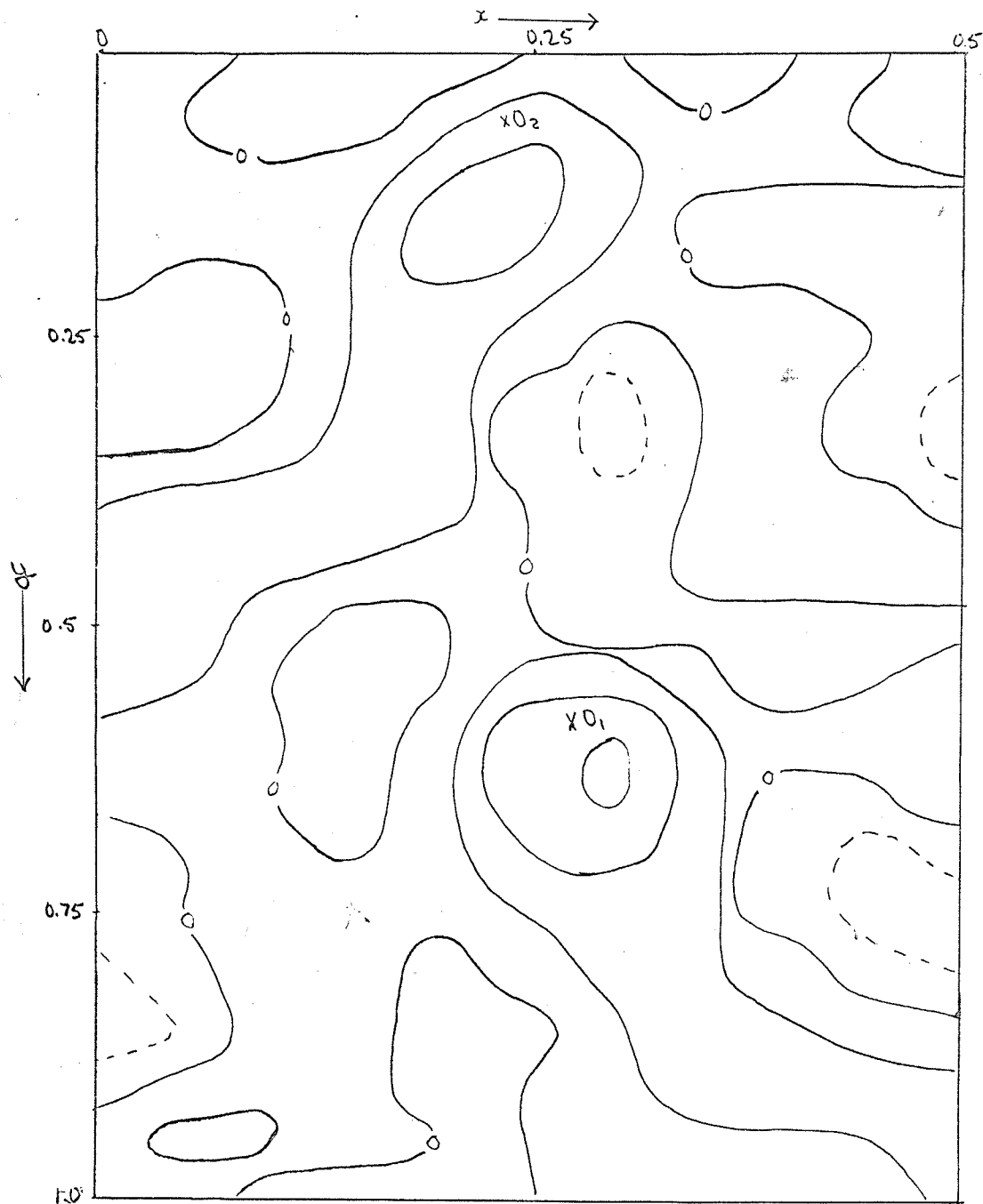
Assumed positions denoted by crosses. Zero and positive contours are solid lines, negative contours are dashed lines.

Figure 6b. Electron density map (F_0 Synthesis) from final structure. x y section at $z = 0.10$. Contour interval $5eA^{-3}$.



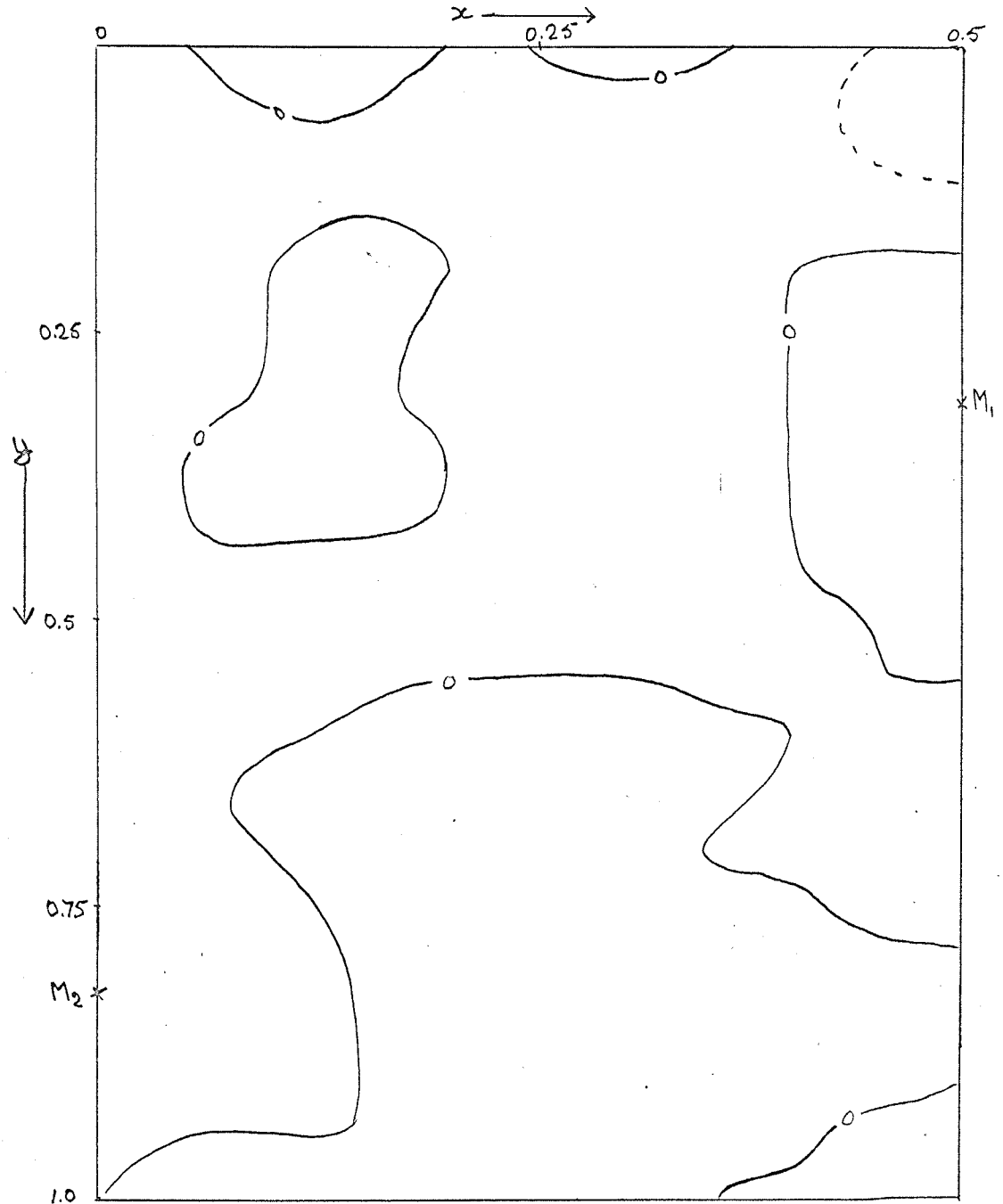
Assumed positions denoted by crosses. Zero and positive contours are solid lines, negative contours are slashed lines.

Figure 6c. Electron density map (F_0 Synthesis) from final structure. x y section at $z = 0.05$. Contour interval $5eA^{-3}$.



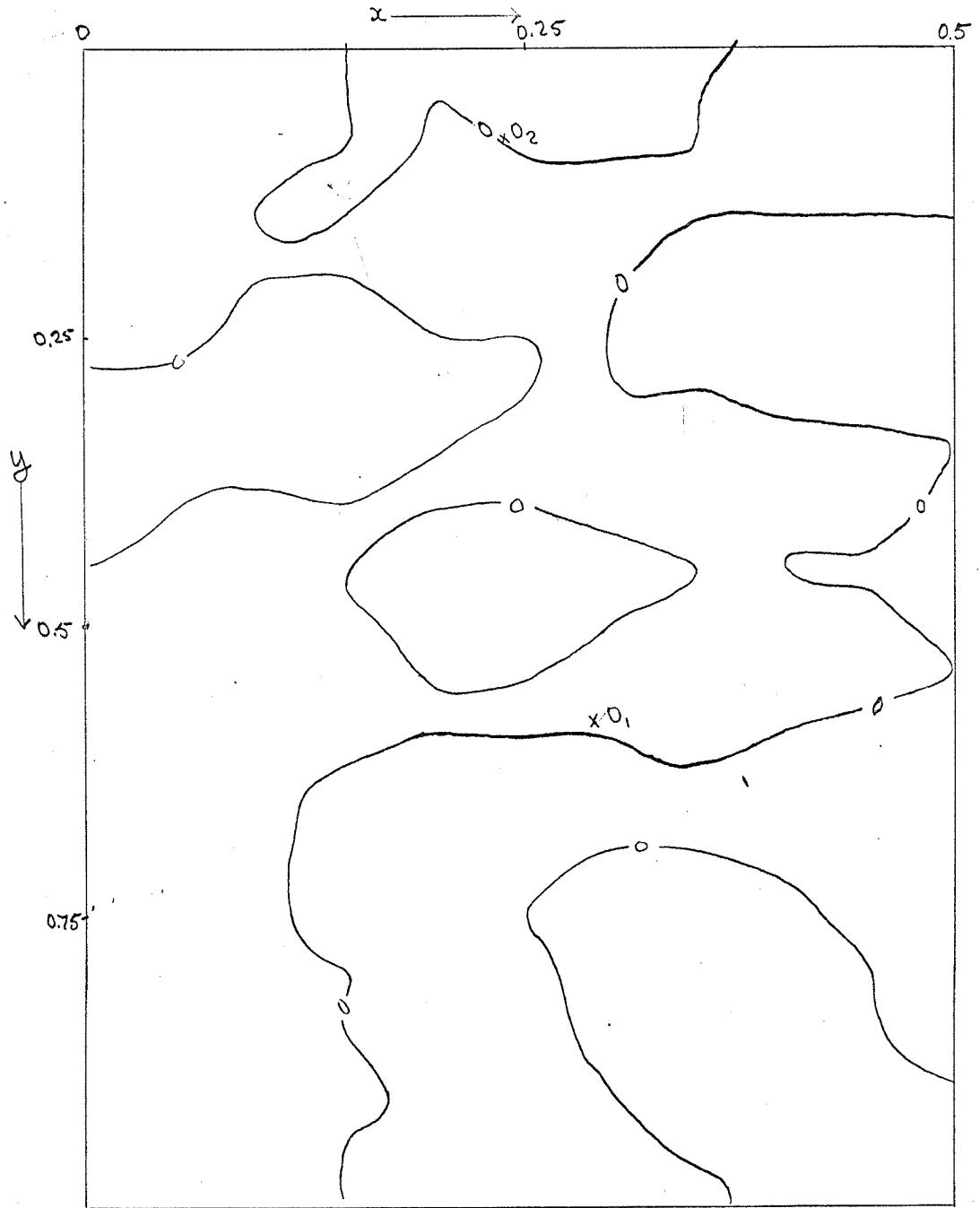
Assumed positions denoted by crosses. Zero and positive contours are solid lines, negative contours are dashed lines.

Figure 7a. Difference map (ΔF Synthesis) from final structure. x y section at $z = 0.25$. Contour interval $5e^{-3}$.



Assumed positions denoted by crosses. Zero and positive contours are solid lines, negative contours are dashed lines.

Figure 7b. Difference map (ΔF Synthesis) from final structure. x y section at $z = 0.10$. Contour interval $5eA^{-3}$.



Assumed positions denoted by crosses. Zero and positive contours are solid lines, negative contours are dashed lines.

Figure 8. Projection along y of the final structure of wodginite.

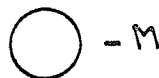
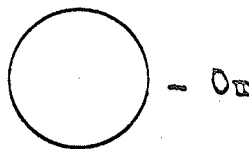
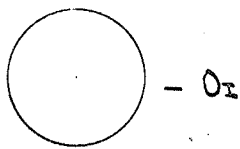
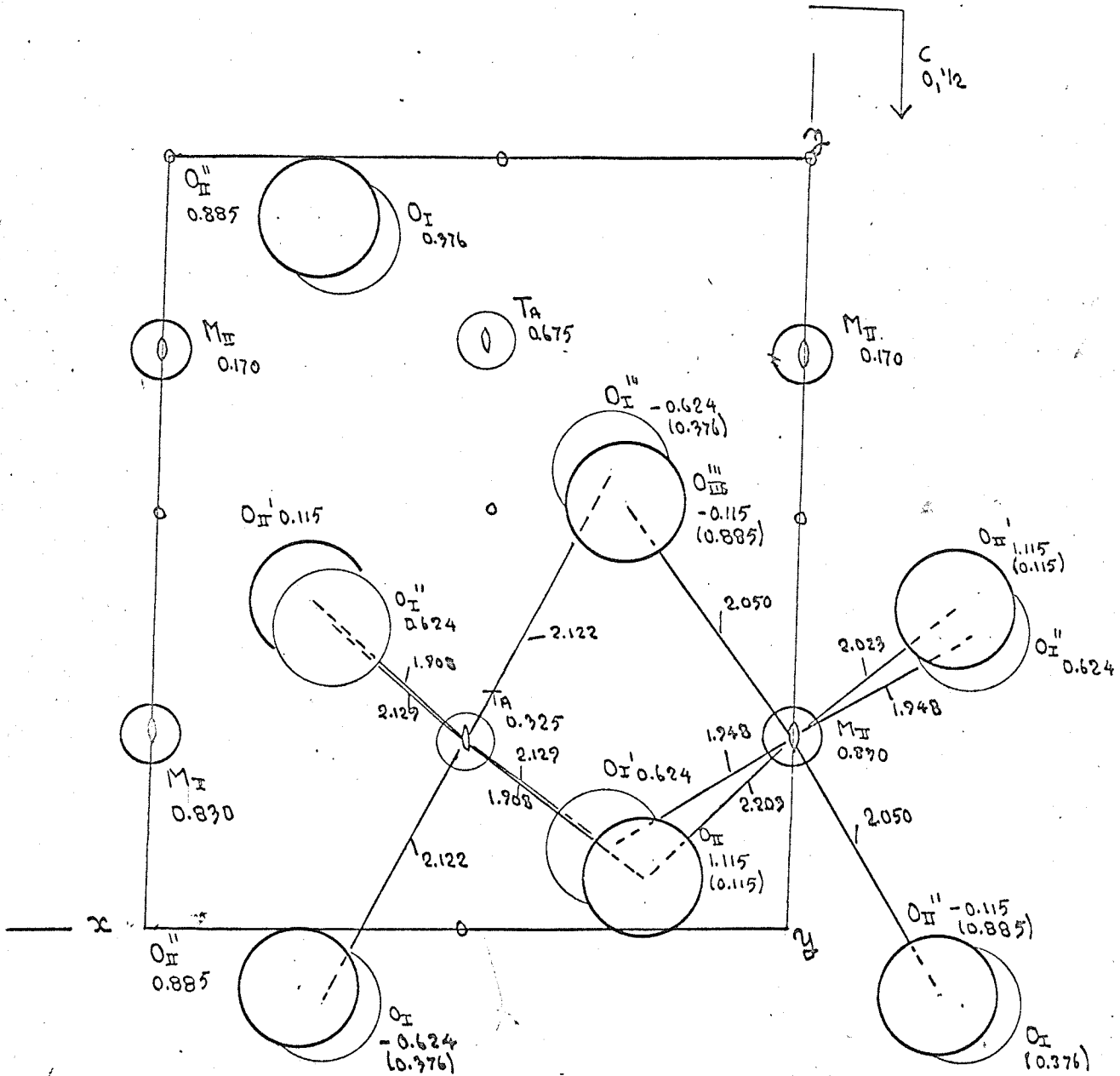


TABLE VIII
BOND LENGTHS

	<u>Bond(A)</u>	<u>St. dev.</u>	<u>Cell.</u>		<u>Bond(A)</u>	<u>St. dev.</u>	<u>Cell.</u>
TA _I -O _I	2.122	0.055	0 0-1	O _I '-O _I ''	2.924	0.056	0 0-1
-O _I '	2.129	0.056	0 0 0	-O _I	2.743	0.111	0 0-1
-O _I ''	2.129	0.056	0 0 0	-O _I '	2.532	0.108	0 0 0
-O _I '''	2.122	0.055	0 0 0	-O _I ''	2.924	0.056	0 0 0
-O _{II}	1.908	0.054	0 0 0	-O _{II} '	2.863	0.075	0 0-1
-O _{II} ''	1.908	0.054	0 0 0	-O _{II} ''	2.853	0.078	0 0 0
				-O _{II} '	2.924	0.088	0 0 0
				-O _{II} ''	2.818	0.088	0 1 0
M _I -O _I ''	1.948	0.056	-1 0 0	O _{II} '-O _I ''	2.853	0.078	0 0-1
-O _I '	1.948	0.056	0 0 0	-O _I	2.863	0.075	0 0-1
-O _{II} '	2.050	0.047	-1 0-1	-O _{II} '	2.793	0.097	-1-1-1
-O _{II} ''	2.203	0.058	-1 1 0	-O _{II} ''	2.966	0.089	-1 0 0
-O _{II} '''	2.050	0.047	0 0 0	-O _{II} '''	2.874	0.062	0-1-1
-O _{III}	2.203	0.058	0 1 0	-O _{II} ''	2.867	0.097	0-1-1
				-O _{III} '	2.874	0.062	0-1 0
				-O _{III} ''	2.959	0.087	0 0 0

Note:- The column headed 'Cell' refers to the cell in which the second atom of the bond is located. Thus in the first bond listed, TA_I-O_I, the O_I atom lies in the cell beneath the cell outlined on the structure diagram as the primary unit cell.

TABLE IX

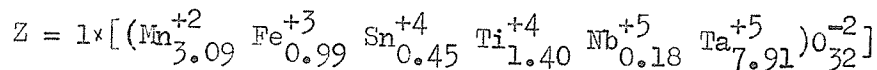
INTERBOND ANGLES

			<u>Bond Angle</u>	<u>St. Dev.</u>	
O_{I}^{III}	(0,0,0)- Ta (0,0,0) -	O_{II}^I	(0,0,0)	90.37	2.08
O_{I}^{III}	(0,0,0)- Ta (0,0,0) -	O_{I}^I	(0,0,0)	80.36	2.30
O_{I}^{III}	(0,0,0)- Ta (0,0,0) -	O_{I}^I	(0,0,0)	86.92	1.92
O_{I}^{III}	(0,0,0)- Ta (0,0,0) -	O_{II}^I	(0,0,0)	99.62	2.05
O_{I}^{III}	(0,0,0)- Ta (0,0,0) -	O_{I}^I	(0,0,-1)	164.19	3.11
O_{II}^I	(0,0,0)- Ta (0,0,0) -	O_{I}^I	(0,0,0)	72.98	2.98
O_{II}^I	(0,0,0)- Ta (0,0,0) -	O_{I}^I	(0,0,0)	165.65	2.32
O_{II}^I	(0,0,0)- Ta (0,0,0) -	O_{I}^II	(0,0,0)	92.67	2.31
O_{II}^I	(0,0,0)- Ta (0,0,0) -	O_{II}^I	(0,0,0)	101.68	3.55
O_{I}^I	(0,0,0)- Ta (0,0,0) -	O_{II}^I	(0,0,0)	92.67	2.31
O_{I}^II	(0,0,0)- Ta (0,0,0) -	O_{II}^I	(0,0,0)	165.65	2.32
O_{I}^I	(0,0,-1)-Ta (0,0,0) -	O_{II}^I	(0,0,0)	99.62	2.05
O_{I}^I	(0,0,-1)-Ta (0,0,0) -	O_{I}^II	(0,0,0)	86.92	1.92
O_{I}^I	(0,0,-1)-Ta (0,0,0) -	O_{I}^I	(0,0,0)	80.36	2.30
O_{I}^I	(0,0,-1)-Ta (0,0,0) -	O_{II}^I	(0,0,0)	90.37	2.08
O_{II}^{III}	(0,0,0)- M_{I} (0,0,0) -	O_{I}^I	(0,0,0)	91.03	2.18
O_{II}^{III}	(0,0,0)- M_{I} (0,0,0) -	O_{II}^I	(0,1,0)	84.92	1.71
O_{II}^{III}	(0,0,0)- M_{I} (0,0,0) -	O_{II}^I	(-1,0,0)	81.99	1.98
O_{II}^{III}	(0,0,0)- M_{I} (0,0,0) -	O_{I}^II	(-1,0,0)	99.72	2.19
O_{I}^I	(0,0,0)- M_{I} (0,0,0) -	O_{II}^I	(0,0,0)	85.27	2.20
O_{II}^I	(-1,1,0)- M_{I} (0,0,0) -	O_{I}^II	(-1,0,0)	85.27	2.20
O_{II}^{II}	(-1,0,-1) M_{I} (0,0,0) -	O_{I}^I	(0,0,0)	99.72	2.19
O_{II}^{II}	(-1,0,-1)- M_{I} (0,0,0) -	O_{II}^I	(0,1,0)	81.99	1.98
O_{II}^{II}	(-1,0,-1) M_{I} (0,0,0) -	O_{II}^I	(-1,1,0)	84.92	1.71
O_{II}^{II}	(-1,0,-1) M_{I} (0,0,0) -	O_{I}^II	(-1,0,0)	91.03	2.18
O_{I}^I	(-1,0,0)- M_{I} (0,0,0) -	O_{I}^I	(0,0,0)	105.38	3.34
O_{I}^II	(-1,0,0)- M_{I} (0,0,0) -	O_{II}^I	(0,1,0)	168.19	2.14
O_{I}^I	(0,0,0) - M_{I} (0,0,0) -	O_{II}^I	(-1,1,0)	168.19	2.14
O_{II}^{II}	(-1,0,-1) M_{I} (0,0,0) -	O_{II}^{III}	(0,0,0)	162.27	3.75
O_{II}^I	(-1,1,0)- M_{I} (0,0,0) -	O_{II}^I	(0,1,0)	84.63	2.92

CHAPTER IV

SUMMARY AND CONCLUSIONS1) Summary.

The wodginite investigated in this study was obtained from the Chemalloy (Tanco) pegmatite at Bernic Lake, Manitoba. The sub-cell with cell dimensions $\underline{a}' = 4.758 \text{ \AA}$, $\underline{b}' = 5.726 \text{ \AA}$, $\underline{c}' = 5.112 \text{ \AA}$ and space group $\underline{P2/c}$, was used for the structure analysis. This sub-cell has one quarter the volume of the real cell and has one quarter the cell content of the real cell, which has cell dimensions $\underline{a} = 9.516 \text{ \AA}$, $\underline{b} = 11.452 \text{ \AA}$, $\underline{c} = 5.112 \text{ \AA}$ and space group $\underline{C2/c}$; its cell volume is 557 \AA^3 . The cell content of the real cell is



Intensity data were collected using an integrating precession camera and a densitometer. The set of computer programs, which are described in the text, were used together with an I.B.M 360/65 computer to carry out the structure analysis on 190 reflections.

The starting structure was based on that of columbite-tantalite described by Sturdivant (1930). From crystallographic and chemical considerations it was decided that one third of the tantalite cell should be taken as the first assumed structure for wodginite. There was a choice of two possible origins, either A or B in Fig. 1a. Origin B was arbitrarily chosen.

The structure was analysed by least squares and Fourier analyses and ultimately refined to give a final R factor of 10.5%.

The final structure proved to be related fairly closely to the tantalite structure as far as the metal atoms were concerned, but the positions of the oxygen atoms in the final structure of wodginite bear

no clear relationship to the positions of those in the tantalite structure.

For the final structure, the parameters, bond lengths and inter-bond angles are given in Tables VII, VIII, and IX respectively, and the final structure is shown in Fig. 8.

2) Conclusions.

- 1) The structure of wodginite is close to that of tantalite (Sturdivant, 1930) apart from the oxygen positions.
- 2) In the sub-cell used, all the Ta atoms are ordered into one metal site (M_1), and all the other metal atoms (Mn, Sn, Ti, Fe, Nb) into the other (M_2) site.
- 3) Each of the two metal sites are pseudo-octahedrally coordinated by oxygens with $M_1(\text{Ta})-\text{O}$ from 1.908 to 2.129 Å and $M_2-\text{O}$ from 1.948 to 2.203 Å. O-O distances around $M_1(\text{Ta})$ vary from 2.532 to 2.924 Å, and around M_2 from 2.793 to 2.966 Å.

3) Reccommendations.

- 1) That the structure of wodginite be refined on the true cell to look particularly for possible ordering of the atoms in the M_2 site. A study of this nature is at present being undertaken by Grice at the University of Manitoba.
- 2) That an interpretation of the refined structure on the true cell be considered in terms of electrostatic charge distributions.

APPENDIX IDERIVATION OF ABSORPTION CORRECTIONS

If the intensity of the X-ray beam incident upon the crystal is given by I_0 , and I is its intensity after traversing a thickness t of the crystal, then

$$I = I_0 e^{-\mu t},$$

where μ is the linear absorption coefficient for the substance in question.

The linear absorption coefficient μ is calculated from the relation

$$\mu = G(\mu/\rho),$$

where G is the density of the crystal, and μ/ρ is the mass absorption coefficient of the crystal. For wodginite, the calculated density is 7.81 gm/cc. (Chapter I, Section (2)), and the mass absorption coefficient is given by

$$\begin{aligned} \mu/\rho = & (p_{\text{Mn}}(\mu/\rho)_{\text{Mn}} + p_{\text{Fe}}(\mu/\rho)_{\text{Fe}} + p_{\text{Sn}}(\mu/\rho)_{\text{Sn}} + p_{\text{Ti}}(\mu/\rho) + p_{\text{Ta}}(\mu/\rho)_{\text{Ta}} \\ & + p_{\text{Nb}}(\mu/\rho)_{\text{Nb}} + p_{\text{O}}(\mu/\rho)_{\text{O}}). \end{aligned}$$

where p_{Mn} is the fraction by weight of the manganese in wodginite, etc., and $(\mu/\rho)_{\text{Mn}}$ is the mass absorption coefficient of manganese, which is given in International Tables for X-ray Crystallography, Vol. 3. The calculations for wodginite are given in Table AI.1 below and for further explanation of absorption effects see Buerger (1960, pp. 204).

Absorption corrections are most easily calculated when the crystal is in the form of a sphere, which was the case for wodginite. The corrections were made in the 'Dataps' program. The value μR given in the input of this program, is just the linear absorption coefficient for wodginite multiplied by the radius R of the spherical crystal which

was used.

μ was found to be 493.36 cm^{-1} as deduced in Table AI.1 below. The diameter of the crystal was measured with a travelling microscope and found to be $0.286 \pm 0.002 \text{ mm}$. Thus, $R = 0.143 \text{ mm} = 0.0143 \text{ cm}$.

Therefore, $\mu R = 0.0143 \times 493.36$

$$= 7.055.$$

Absorption corrections for this value of μR for a spherical crystal were obtained from the International Tables for X-ray Crystallography, Vol. 2, page 299, for various values of $\sin\theta$.

TABLE AI.1
CALCULATION OF LINEAR ABSORPTION COEFFICIENT
FOR WODGINITE

<u>Atom</u>	<u>Atomic Weight</u>	<u>Total weight of</u>	<u>Fraction of Total</u>
		<u>atom in species.</u>	<u>Weight, p.</u>
Mn	54.93	0.96 54.93 = 52.73	8.118 %
Fe	55.85	0.09 55.85 = 5.03	0.774
Sn	118.70	0.59 118.70 = 70.03	10.781
Ti	47.90	0.22 47.90 = 10.30	1.586
Ta	180.88	2.11 180.88 = 381.30	58.701
Nb	92.91	0.02 92.91 = 2.14	0.330
O	16.00	8.00 16.00 = <u>128.00</u>	<u>19.706</u>
		649.53	99.996

For Mo k_{α} radiation

<u>Atom</u>	<u>(μ/ρ)</u>	<u>$p(\mu/\rho)$</u>
Mn	34.7 gm ⁻¹	281.70 gm ⁻¹ 10 ⁻²
Fe	38.5 "	29.80 " "
Sn	31.1 "	335.29 " "
Ti	24.2 "	38.38 " "
Ta	95.4 "	5600.08 " "
Nb	17.1 "	5.64 " "
O	1.3 "	<u>25.82</u> " "
		6316.71 gm ⁻¹ 10 ⁻²

Therefore,

$$\mu = 7.81 \times 63.17 \text{ cm}^{-1}$$

$$\mu = 493.36 \text{ cm}^{-1}$$

N.B. The atomic proportions of the elements used here (0.96, 0.09, etc.) differ somewhat from those given in the formula on p.5 because initially, when the absorption coefficients were calculated, one analysis of Grice's (1970) for this specimen was used, whereas later in the study another analysis of his was regarded as preferable. The second analysis is the one given in Table I and used throughout the thesis except in Table AI.1.

APPENDIX II
DETERMINATION OF ACCURATE CELL DIMENSIONS
BY THE PRECESSION METHOD

Measurements of the separations between the principal reciprocal lattice planes, X_i , $i = 1, 2, 3$, as represented on the precession photographs (i.e. the true separation multiplied by a magnification factor, F , the crystal-to-film distance) were made in the usual way (Buerger, 1964) such that,

$$X_1 = d^*(100) F, X_2 = d^*(010) F, X_3 = d^*(001) F.$$

After developing, X-ray films have a tendency to shrink to a different extent in the two directions parallel to the edges of the film. This clearly will effect the values of X_i obtained from the photographs. To compensate for this effect, the distance between the two fiducial spots on the film cassette, S , was measured. Before developing but after exposure of a film, the cassette was opened in a dark room, the film turned through 90° and replaced in the cassette. The closed cassette was exposed to light and the film developed in the usual way. Thus the fiducial spots were recorded on the film in both the horizontal and vertical directions. These two distances, S_{mh} and S_{mv} , were measured on the developed film. The appropriate ratio of S/S_m when multiplied by X_i , then gives the value which X_i would have taken if there had been no shrinkage.

The real lattice period, A_i , can then be expressed as

$A_i = \lambda F S_m / X_i S$, where λ is the wavelength of the radiation used.

The camera was calibrated using a quartz crystal and measuring the X separations on the photograph corresponding to the reciprocal

period d $[111]_F$ (rhombohedral axes). Thus, A_o , the direct spacing which corresponds to d (111) can be expressed as

$$A_o = \lambda FS_{mo} / X_o S.$$

Combining the two expressions for A_i and A_o , we have

$$A_i = X_o S_m A_o / X S_{mo} \quad (1)$$

Thus λ has been eliminated from the calculations and the final value of A_i calculated from equation (1) is corrected for film shrinkage.

APPENDIX III
INPUT FORMATS FOR COMPUTER PROGRAMS

1) 'Precroc'

As an example of the input format for this program, the data for the h0L level of wodginite are given here with explanations of the meaning of the input variables.

- cc Card 1 (Title card)
- 1-80 WODGINITE
- Card 2 (System card)
- 1-80 MONOCLINIC H POSITIVE (Crystal system of wodginite-
all reflection indices must be entered with their
h indices positive.)
- Card 3 (Absences card)
- 1-80 HOL, L = 2N (Simple statement of systematic absences
for the space group of the crystal.)
- Card 4 (Control card)
- 1-3 bb4 (NFILM - Number of films in this level which
are to be processed.)
- 4-6 bb0(KRAT - this is equal to zero if the intensity
ratios from film to film are to be computed; it is
equal to non-zero if these ratios are already known
and can be entered as input data on card 7)
- 7-9 bb2 (MULT - Multiplicity of reflections which occur
on this level; in general the multiplicity of the
hkL reflections in the monoclinic system will be 4,
but in certain cases this reduces to 2 because
 $I_{hkL} = I_{\bar{h}kL} = I_{h\bar{k}L} = I_{\bar{h}\bar{k}L}$.)

13-15 bb2 (IFUN- With this variable set equal to 2, the final intensity value for each reflection listed in the output and that which is written on disk ready for input into the next program will be, for say the hkL reflections, the average value of the hkL , $\bar{h}\bar{k}\bar{L}$, $\bar{h}k\bar{L}$, $h\bar{k}L$ reflections.)

Card 5 (Heading card)

1-11 H0L (These headings are just names which can be applied to
12-22 $\bar{H}\bar{O}\bar{L}$ each set of symmetry-related reflections.)

Card 6 (Intensity parameters card)

1-6 1.0 (Output scale factor - final output can be scaled up or down according to this factor)

7-12 600.0 (Upper limit of intensity : any intensity with a value greater than this upper limit of 600 was given a zero weight and thus excluded from any ratio or scaling calculations.)

13-18 15.0 (Threshold value- this is the minimum value assigned to an intensity; in the case of wadginite any value which was entered into the program with a value of less than 15.0 was automatically assigned the threshold value.)

Card 7 (Ratios card)

This card is only relevant when predetermined ratios are used cross-scaling the films, which was not the case here.

Card 8 (Reflection card)

1-4 H

5-8 K

9-12 L

13-18 Intensity on first film.

19-24 Intensity on the second film; etc.

One card 8 is entered for each reflection recorded on this level.

Card 9 (Sentinel card)

80 1 - End of information.

2 - New set of data starting with a title card.

The program first finds one weighted and scaled value for each reflection from the four separate values that have been entered. Then it averages out the intensities for each group of symmetry-related reflections.

2) 'Dataps!'

As an example of the input format for this program the data for the OkL level of wodginite are given here.

cc

Card 1 (Title card)

2-80 WODGINITE OKL

Card 2 (Reciprocal cell dimensions)

1-9 0.2105 (a = $1/d(100)$)

10-18 0.1748 (b = $1/d(010)$)

19-27 0.1956 (c = $1/d(001)$)

28-36 0.0 ($\cos\alpha = -\cos\alpha$ for $\alpha = \alpha = 90^\circ$)

37-45 0.05432 ($\cos\beta = -\cos\beta$ for $\beta = \beta = 91^\circ 08'$)

46-54 0.0 ($\cos\gamma = -\cos\gamma$ for $\gamma = \gamma = 90^\circ$)

Card 3 (Transformation matrix from cell axes to internal axes)

Card 3a

15- 1.0 (The first of these cards represents the precession axis,
 25- 0.0 in this case a or [100])
 35- 0.0

Card 3b

1- (The second of these cards represents the rotation axis,
 15- 0.0 in this case z or [001])
 25- 0.0
 35- 1.0

Card 3c

15- 0.0 (The third card represents the second reciprocal axis
 25- 1.0 lying in the plane of the zero-level film, in this case
 35- 0.0 y, which is in the monoclinic case equivalent to y or
 [010])

Card 4 (Grid card)

This card is not applicable when spherical absorption routine
 is being used.

Card 5

Blank card.

Card 7

Blank card.

Card 8 (Reflection batch card)

1-5 1 (Index number of level.)
 6-15 0.71069 (Wavelength of X-radiation used, in this case that for
 MoK α .)
 36-45 1.0 (Overall scale factor. The program will multiply all F_{obs}
 values by this scale factor.)

46-50 5.0 (Intensity threshold value, i.e. the minimum intensity value to be included.)

50-55 25.0 (Precession angle used when recording this level of photographs.)

56-65 90 (Minimum angle at which splitting of spots occurs. On integrated precession photographs this phenomenon is not observed.)

71-75 11 (NFI - logical number of input tape.)

76-80 15 (NTO - logical number of output tape.)

Card 9 (Absorption correction for a sphere)

1-76 457.371.251.169.121.90.470.456.747.039.834.430.226.924.322.
320819.719.018.7 (19 values for URT, absorption corrections for theta from the International Table, Vol.2 page299, for the value of μR calculated in Appendix I.

76-80 7.06 (R - absorption coefficient times the radius of sphere.)

Card 10

1-3 H

4-6 K

7-9 L

10-19 I_{obs}

20-29 WEIGHT

30-39 Scale factor for observed intensities.

Card 10 is only relevant when the reflection data are being read from cards. When the reflection data are being read from the disk storage produced by 'Precproc', as was the case with wodgeinite, all card 10's may be omitted but the rest of the batch must be put in as usual.

When further reflection data are to be fed in from reciprocal levels parallel to OkL , i.e. those precessing about the same axis, only cards 1, 8 and 9 need be repeated before each successive batch of reflection data. However, when data from levels which are not parallel to OkL , i.e. those not precessing about the same axis as OkL , are to be fed in, all the cards must be repeated for the first level precessing around this new axis and so on for each new batch with a different precession axis.

3) 'Genles'

As an example of the input format for this program, the partial data for one run for wodginite are given here.

Card 1 (Run identification card)

1-72 WODGINITE LEAST SQUARES NO. 1

Card 2 (Run control card)

1-4 4 (No. of atomic positions to be read in.)
 5-8 0
 9-12 0
 13-16 1 (Denotes a non-standard data tape to be read in)
 17-20 1 (Cell dimensions to be read in from card 3.)
 21-24 1 (Space group to be read in from standard data tape.)
 25-28 3 (Number of different types of form factor cards to be read
 in: 1 for oxygen, 1 for tantalum and one for the 'mixed atom'.)
 29-32 0
 33-36 0
 37-40 3 (Weight of F_{obs} calculated from the relationship

$$w = 1/(F_{\text{obs}} + 0.02 F_{\text{obs}})^{1/2}$$

41-44 0

45-48 0 (Use weighting scheme specified in col 37-40.)

49-52 0 (Allow only positive values for β or β_{ij} , the temperature factors.)

53-56 1

57-60 1 (Assume extinction not present.)

61-64 0

65-68 1 (Hold constant all data scale factors.)

69-72 0

73-76 40 (Only data with $\sin^2\theta/\lambda^2$ less than 40/100 will be taken from data tape.)

77-80 -1 (Output of debugging information.)

Card 3 (Unit cell and X-ray wavelength)

1-10 4.758 (a A)

11-20 5.726 (b A)

21-30 5.112 (c A)

31-40 90.0 (α°)

41-50 91.10 (β°)

51-60 90.0 (γ°)

67-70 0.71069 (λ A)

Card 4 (Space group symbol)

1-80 P2/c

Card 5 (Non-standard data tape control)

1-4 1 (BCD data tape)

5-8 0 (IRSK - number of initial records on the tape to be skipped over and ignored.)

- 12 0 (JFXHKL - this is zero if we have a binary tape and hkl floating point numbers.)
- 13-16 1 (JH - serial number of h as it appears in record.)
- 17-20 2 (JK - serial number of k as it appears in record.)
- 21-24 3 (HL - serial number of L as it appears in record.)
- 25-28 0 (JSQ - program will compute $\sin^2\theta/\lambda^2$.)
- 29-32 0 (JPL - $\beta(2\theta)$ absent from data.)
- 33-36 4 (JF - serial number of F_{obs} .)
- 37-40 0 (JFSQ - F_{obs}^2 absent from data.)
- 41-44 -5 (JW - serial number of $\sigma(F)$ in record. Negative sign indicates that $\sigma(F)$ is to be read and not $1/\sigma_{F_{\text{obs}}}$.)
- 45-48 0 (JSIG - $\sigma(F^2)$ absent from record.)
- 49-52 0 (JNI - all data from this tape and no scale indication is given in records.)
- 53-56 2 (LSTH - h for last reflection on this tape.)
- 57-60 2 (LSTK - k for last reflection on this tape.)
- 61-64 -5 (LSTL - L for last reflection on this tape.)
- 65-68 8 (IRCL - total number of items in the record.)
- 69-72 0
- 73-76 880 (IF00 - F_{000} .)
- 77-80 15 (ITAPE - Fortran reference number for the tape.)
- Card 6 (Format for non-standard data tape.)
- 1-80 (3F9.0,2F9.3,F9.0,F10.2,F10.6)
- Card 7 (Form factor cards. Form factors taken from tables to be found in Act. Cryst. A24 321, 1968.)

The form factor card for oxygen is shown below, the tantalum and 'mixed atom' cards follow the same form.

2-7 OXYGEN
 10-16 3.225630
 17-23 18.499100
 24-30 3.017170
 31-37 6.656799
 38-44 1.425529
 45-51 0.405890
 52-58 0.905250
 59-65 61.188889
 66-72 0.423620

N.B. The form factor used for the 'mixed atom' was weighted average of form factors for Mn, Fe, Ti, Sn, Nb and Ta.

Each form factor card must be followed by a blank card.

Card 9 (Atomic parameters card)

Card 9a

1-10 x/a (Atomic coordinates.)
 11-20 y/b (Atomic coordinates.)
 21-30 z/c (Atomic coordinates.)
 31-40 β (β isotropic.)
 43 n_i (serial number of atomic form factor, e.g. 1 for oxygen,
 2 for tantalum and 3 for the 'mixed atom'.)
 50 0 (Isotropic β is to be read in.)
 1 (Anisotropic β_{ij} are to be read in on following card 9b.)
 51 0 (No refinement of occupancy parameter, p.)
 1 (Refinement of occupancy parameter, p.)
 52 0 (Refine x)
 1 (Hold x constant.)

- 53 0 (Refine y.)
 1 (Hold y constant.)
- 54 0 (Refine z.)
 1 (Hold z constant.)
- 55 0 (Refine β .)
 1 (Hold β constant.)
- 56-65 p (Occupancy parameter, p, is equal to 0.0 for total occupancy.)
Card 9b (Anisotropic temperature factors card.)

One card 9 must be entered for each atom i.e. four in all.

Card 10 (Refinement cycle control card)

4) 'Fourier'

The input format given below is that used for an F_o synthesis of wadginite. Where alterations are necessary for a difference synthesis, they are noted.

Card 1

- 15 10 (Maximum h)
 20 10 (Maximum k)
 25 10 (Maximum L)
 30 3 (z-sections will be produced.)
 35 1 (For F_{obs} Fourier.)
 3 (For ΔF Fourier.)
 40 -1 (Data tape is read from 'Genles' output.)
 45 11 (Logical number of input tape.)

Card 2

1-72 P 2 / c

Card 3 (Run identification card)

1-80 TWO DIMENSIONAL FOURIER

Card 4

5 20 (Number of cell divisions in X-direction)
10 20 (Number of cell divisions in Y-direction)
15 20 (Number of cell divisions in Z-direction)
20 0 (X origin)
25 0 (Y origin)
30 0 (Z origin)
35 11 (Number of points in X)
40 21 (Number of points in Y)
45 11 (Number of points in Z)
46-55 125 (Volume of unit cell in A^3)

REFERENCES

- BARNES, W.H (1949): Some Comments on the Buerger Precession Method for the Determination of Unit Cell Constants and Space Groups. *Am. Mineral.* 34, 174-180
- BARNES, W.H., PRZYBYLSKA, M., AND SHORE, V.C. (1951): Further Notes on the Precision of the Buerger Precession Instrument. *Am Mineral.*, 36, 430-435.
- BOURGUIGNON, P. ET MELON, J. (1965): Wodginite du Rwanda. *Ann. Soc. Geol. de Belgique*, t. 88, 291-300.
- BUERGER, M.J. (1960): *Crystal Structure Analysis*. Wiley.
- BUERGER, M.J. (1964): *The Precession Method*. Wiley.
- GRICE, J. (1970): The Nature and Distribution of the Tantalum Minerals in the Tanco(Chemalloy) Mine Pegmatite at Bernic Lake, Manitoba. M.Sc. Thesis, University of Manitoba.
- GRICE, J., CERNY, P. AND FERGUSON, R.B. (1972): The Tanco Pegmatite at Bernic Lake, Manitoba II. Wodginite, Tantalite, Pseudo-Ixiolite and Related Minerals. *Canadian Mineral.*
- KHVOSTOVA, V.A. ET AL (1965): The First Find of Wodginite in the U.S.S.R. (Translation). *Dokl. Acad. Sci. U.S.S.R., Earth Sci. Sect.*, v. 167, 109-112.
- von KNORRING, O. (1968): On the Geochemistry of some Niobium-Tantalum Minerals from African Pegmatites. 12th. Ann. Rept. *Inst. African Geol., Univ. Leeds*, 50-53.
- von KNORRING, O., SAHAMA, T.G. AND LEHTINEN, M. (1969): Ferroan Wodginite from Ankole, Southwest Uganda. *Bull. Geol. Soc. Finland* 41, 65-69.

- LUNA, J. (1965): Wodginite and Columbite-tantalite from a Pegmatite at Krasonice (Western Moravia). Acta. Univ. Carolinae, Geologica No. 3, 157.
- NICKEL, E.H., ROWLAND, J.F. AND McADAM, R.C. (1963a): Wodginite a new Tin-manganese Tantalite from Wodgina, Australia and Bernic Lake, Manitoba. Can. Min., 7, 390-402.
- PATTERSON, A.L. AND LOVE, W.E. (1960): Error Analysis for the Buerger Precession Camera. Am. Min. 45, 325-333.
- STURDIVANT, J.H. (1930): The Crystal Structure of Columbite. Z. Krist. 75, 88-108.
- VORMA, A., AND SIIVOLA, J. (1967): Sukulaite-Ta₂Sn₂O₇- and Wodginite as Inclusions in Cassiterite in the Granite Pegmatite in Sukula, Tammela in SW Finland. C.R. Soc. geol. Finlande, 39, 173-187.